Quaternary Geochronology 72 (2022) 101278

Contents lists available at ScienceDirect

Quaternary Geochronology

journal homepage: www.elsevier.com/locate/quageo

# Dating basal peat: The geochronology of peat initiation revisited

Cindy Quik [a,*], Sanne W.L. Palstra [b], Roy van Beek [a,c], Ype van der Velde [d], Jasper H.J. Candel [a], Marjolein van der Linden [e], Lucy Kubiak-Martens [e], Graeme T. Swindles [f,g], Bart Makaske [a], Jakob Wallinga [a]

[a] Soil Geography and Landscape Group, Wageningen University & Research, Wageningen, the Netherlands
[b] Centre for Isotope Research, Energy and Sustainability Research Institute Groningen, University of Groningen, Groningen, the Netherlands
[c] Cultural Geography Group, Wageningen University & Research, Wageningen, the Netherlands
[d] Faculty of Science, Earth and Climate, Vrije Universiteit Amsterdam, Amsterdam, the Netherlands
[e] BIAX Consult, Zaandam, the Netherlands
[f] Geography, School of Natural and Built Environment, Queen's University Belfast, Belfast, United Kingdom
[g] Ottawa-Carleton Geoscience Centre and Department of Earth Sciences, Carleton University, Ottawa, Ontario, Canada

ARTICLE INFO

*Keywords:*
Accelerator mass spectrometry (AMS)
Bulk
Humics
Humins
Organic matter
Peat initiation
Peat remnant
Plant macrofossils
Radiocarbon
Stratigraphy

ABSTRACT

Attributing the start of peat growth to an absolute timescale requires dating the bottom of peat deposits overlying mineral sediment, often called the *basal peat*. Peat initiation is reflected in the stratigraphy as a gradual transition from mineral sediment to increasingly organic material, up to where it is called peat. So far, varying criteria have been used to define basal peat, resulting in divergent approaches to date peat initiation. The lack of a universally applicable and quantitative definition, combined with multiple concerns that have been raised previously regarding the radiocarbon dating of peat, may result in apparent ages that are either too old or too young for the timing of peat initiation. Here, we aim to formulate updated recommendations for dating peat initiation. We provide a conceptual framework that supports the use of the organic matter (OM) gradient for a quantitative and reproducible definition of the mineral-to-peat transition (i.e., the stratigraphical range reflecting the timespan of the peat initiation process) and the layer defined as *basal peat* (i.e., the stratigraphical layer that is defined as the bottom of a peat deposit). Selection of dating samples is often challenging due to poor preservation of plant macrofossils in basal peat, and the representativity of humic and humin dates for the age of basal peat is uncertain. We therefore analyse the mineral-to-peat transition based on three highly detailed sequences of radiocarbon dates, including dates of plant macrofossils and the humic and humin fractions obtained from bulk samples. Our case study peatland in the Netherlands currently harbours a bog vegetation, but biostratigraphical analyses show that during peat initiation the vegetation was mesotrophic. Results show that plant macrofossils provide the most accurate age in the mineral-to-peat transition and are therefore recommendable to use for $^{14}$C dating basal peat. If these are unattainable, the humic fraction provides the best alternative and is interpreted as a terminus-ante-quem for peat initiation. The potential large age difference between dates of plant macrofossils and humic or humin dates (up to ~1700 years between macrofossil and humic ages, and with even larger differences for humins) suggests that studies reusing existing bulk dates of basal peat should take great care in data interpretation. The potentially long timespan of the peat initiation process (with medians of ~1000, ~1300 and ~1500 years within our case study peatland) demonstrates that choices regarding sampling size and resolution need to be well substantiated. We summarise our findings as a set of recommendations for dating basal peats, and advocate the widespread use of OM determination to obtain a low-cost, quantitative and reproducible definition of *basal peat* that eases intercomparison of studies.

## 1. Introduction

The start of peat growth represents a major landscape change. Attributing this transition to an absolute timescale requires dating the bottom of peat deposits overlying mineral sediment, often called the *basal peat*. Robust age control of basal peat layers is of paramount

* Corresponding author. Wageningen University & Research, Soil Geography and Landscape Group, Postbus 47, 6700 AA, Wageningen, the Netherlands.
*E-mail address:* cindy.quik@wur.nl (C. Quik).

https://doi.org/10.1016/j.quageo.2022.101278
Received 24 November 2021; Received in revised form 15 March 2022; Accepted 21 March 2022
Available online 26 March 2022

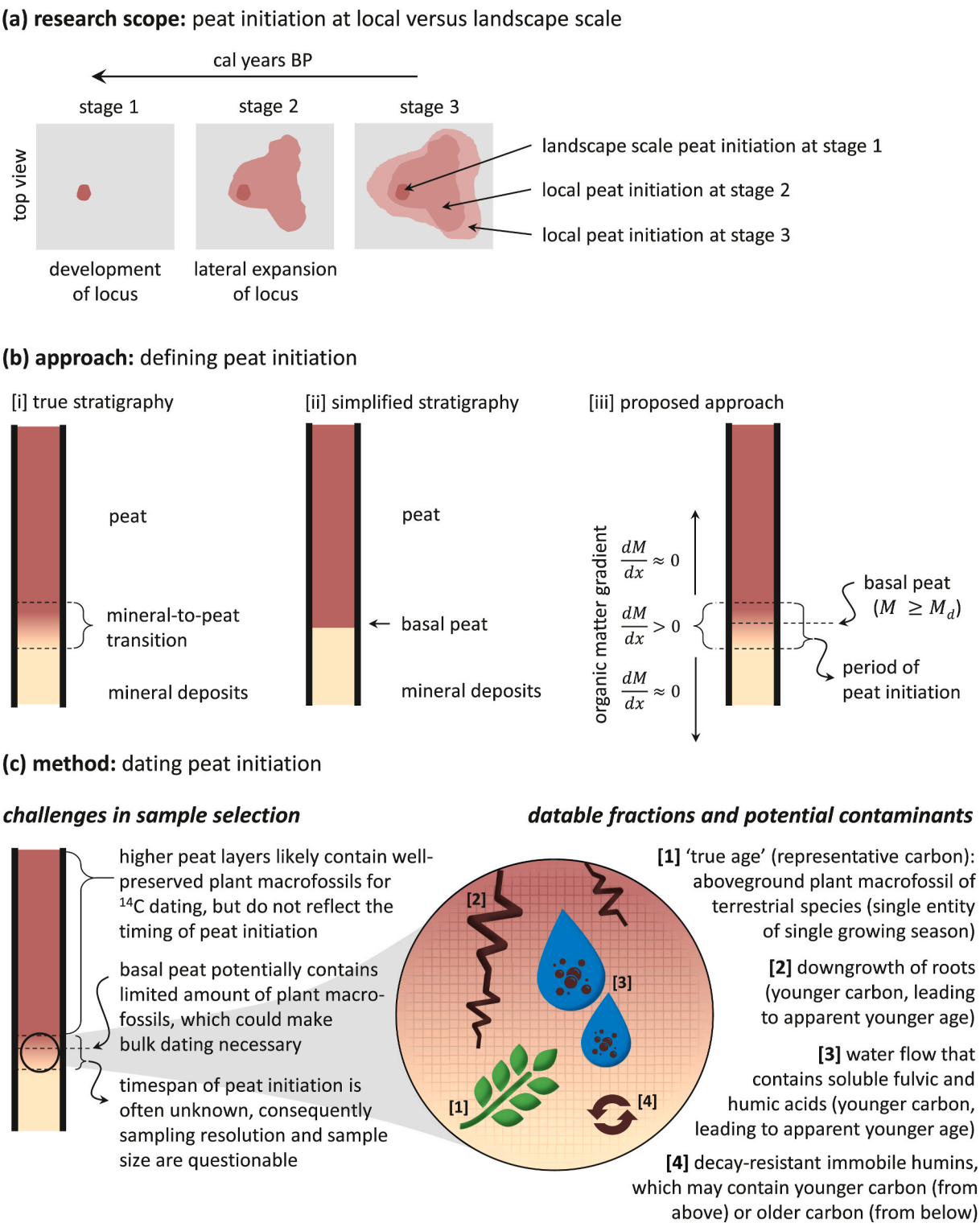


**Fig. 1.** Conceptual framework for dating peat initiation. (a) Schematic top-view of a landscape (peat is indicated in brown), showing the meaning of *peat initiation* at both the landscape and local scales. (b) Schematic cores showing [i] stratigraphy that results from peat initiation, [ii] simplified interpretation of this stratigraphy, and [iii] the approach we propose in this study. Here, we propose using the organic matter gradient to characterise the mineral-to-peat transition and to define *basal peat*. To qualify the material as peat, the OM content should be above a certain value denoted with $M_d$, where the first cm of material that has an OM content equal to or above $M_d$ is defined as the *basal peat*. (c) Schematic core showing challenges with sample selection, and datable fractions and potential contaminants for $^{14}$C dating *basal peat*.

importance, not only for studies aimed directly at peatlands, for instance concerning their palaeogeography, development and carbon sequestration (e.g. Gorham et al., 2007; Yu et al., 2011), but also for interdisciplinary research fields that harness the peat archive for climate and sea level reconstructions (e.g. Törnqvist and Hijma, 2012; Morris et al., 2018) or to contextualise wetland archaeology (e.g. Chapman et al., 2013).

Peat growth results from a positive production-decay balance, i.e.

where the decay rate of organic material is slower than the rate of production. The decay rate primarily depends on moisture level, which in turn is influenced by various factors such as climate (e.g. Weckström et al., 2010), changes in hydrological base level (sea level rise, e.g. Berendsen et al., 2007) or regional groundwater changes (e.g. Van Asselen et al., 2017), landforms and surface topography (e.g. Almquist-Jacobson and Foster, 1995; Mäkilä, 1997; Loisel et al., 2013), impermeable deposits or resistant layers in the soil profile (e.g. Breuning-Madsen et al., 2018; Van der Meij et al., 2018), and anthropogenic influence (e.g. Moore, 1975; Moore, 1993).

A wetland is an area where the substrate is water-saturated or inundated for a substantial period (Charman, 2002a; Joosten and Clarke, 2002). A minimum depth of 30 cm of peat is required to classify a wetland area as a peatland (Charman, 2002a; Joosten and Clarke, 2002; Rydin and Jeglum, 2013a). This implies that during build-up of the first organic deposits, the area is not yet a peatland according to definition, but rather a wetland where peat formation occurs. As a result of these definitions, one could make a distinction between peat initiation (i.e., build-up of the first organic deposits) and peatland initiation (i.e., referring to the moment when 30 cm of organic deposits has formed in a certain area). In the current paper, we focus on peat initiation (prior to the formation of a peat layer with a thickness of 30 cm or more).

Peat initiation may occur through (a combination of) three processes, briefly outlined below based on Charman (2002b) and Rydin and Jeglum (2013b). Terrestrialisation (also called infilling) refers to the process where peat develops in or at the edge of water bodies. Terrestrialisation is characterized by gyttja deposits at the base, which require a water depth of at least 0.5 m to form (Bos, 2010). Paludification refers to peat formation on previously unsaturated mineral substrate, and thus reflects moistening of the landscape. Primary mire formation involves peat growth on newly exposed waterlogged substrate (e.g. after land uplift from sea). Here, peat growth starts directly on the fresh parent material.

When a peat surface rises above the regional groundwater level, consequent strong dependence on rainwater leads to ombrotrophication, which may result in a fen-bog transition (Charman, 2002c; Rydin and Jeglum, 2013b; Loisel and Bunsen, 2020). Peatlands not only grow vertically, but also expand laterally, which results in a larger peat-covered area. Paludification of surrounding soils due to poor drainage at the edge of the peatland, and resulting peatland expansion, is known as an autogenic process (Charman, 2002c). However, allogenic factors such as climate and topography influence the rate and extent of lateral spread (e.g. Korhola, 1994; Ruppel et al., 2013).

Peat initiation can be studied at various scales (Fig. 1a). At the landscape scale, peat initiation refers to the onset of peat growth at a certain locus, that expands over time to cover a larger area. In this case, the term *peat initiation* refers to the location and time where the nucleus of the resultant peatland developed. In contrast, at the very local scale, *peat initiation* may be used to indicate the moment of accumulation of the first peat deposits at a specific location, where the location may reflect a development locus but could also be a site that became covered by peat through lateral expansion of a nearby locus. To distinguish lateral expansion from a development locus, one or multiple transects of basal peat dates are usually required (e.g. Mäkilä, 1997; Mäkilä and Moisanen, 2007; Chapman et al., 2013). The approach for dating peat initiation at both scales is similar, while the research aim determines which scale level is of interest.

Peat initiation is a process that takes place during a certain timespan, which is reflected in the stratigraphy as a gradual transition from mineral sediment to increasingly organic material (Fig. 1b), up to where it is called peat (depending on definitions used). We propose it would be most accurate to speak of a period of peat initiation, which requires a series of vertical dates that encloses the gradual stratigraphical boundary. However, a single date of *basal peat* is often used to reflect peat initiation, potentially for reasons of practicality or feasibility when there is need to date many sites. This requires however an unambiguous and explicit definition of *basal peat*.

**Table 1**
Concerns with $^{14}C$ dating of peat samples. 'Organism' refers to a plant of peat-forming vegetation.

| Processes when the organism was alive | Processes after the organism died |
|---|---|
| *Apparent older age*<br>Circumstances where organisms incorporate carbon from a reservoir that is not in equilibrium with the atmosphere (so-called reservoir effect), causing apparent ages that are too old:<br>• This typically applies to aquatic samples from marine or freshwater circumstances (the latter is also known as hardwater effect, e.g. Törnqvist et al., 1992; Philippsen, 2013). Relevance of a reservoir effect for peat samples has been postulated (Kilian et al., 1995) but not confirmed (Blaauw et al., 2004).<br>Incorporation of older carbon or $^{14}C$-depleted carbon may also occur through:<br>• Decomposition of underlying peat layers and subsequent assimilation of $CO_2$ (Smolders et al., 2001).<br>• Assimilation of $CH_4$ originating from bacterial methanogenesis (Van der Plicht et al., 2019). | *Apparent younger age*<br>Mixing with younger carbon through:<br>• Downgrowth of roots (Törnqvist et al., 1992).<br>• Translocation of mobile humic acids downwards in a profile, followed by chemical break-down to humins (Palstra et al., 2021).<br>• Contamination during sample storage by microbial growth (Wohlfarth et al., 1998) or laboratory pre-treatments. Small samples or samples with low carbon content are particularly sensitive to contamination (Van der Plicht et al., 2019), especially if samples are older than 20 ka. |

So far, varying criteria have been used to define *basal peat*, resulting in divergent approaches to date the onset of peat accumulation (Quik et al., 2021). Current approaches, which are partly dependent on the research objectives, vary from visual determinations and basic laboratory analyses such as loss-on-ignition (e.g. Edvardsson et al., 2014) to detailed micromorphological analyses (e.g. Cubizolle et al., 2007) and studies of plant macrofossils (e.g. Loisel et al., 2013). Depending on the approach taken, the accuracy of resulting dates to represent peat initiation may be called into question, as the (possibly site-specific) definition of the *basal peat* often remains implicit.

The international soil classification of the World Reference Base for Soil Resources states that 'organic material' has $\geq$20% soil organic carbon in the fine earth fraction (by mass) (WRB-IUSS, 2015). A practical challenge of this definition is that determination of soil organic carbon requires expensive analyses (e.g. elemental analysis), whereas soil organic matter (which includes both organic carbon and, if present, inorganic carbon such as carbonates) can be measured with an inexpensive, simple protocol (loss-on-ignition).

To the best of our knowledge, both the mineral-to-peat transition and the layer called *basal peat* (the stratigraphical level used to reflect peat initiation), are not universally defined based on organic matter (OM) content. A universal definition eases inter-site comparisons, but a site-specific definition may be preferable to cover regional differences. Both require that the properties to define *basal peat* are explicit and reproducible. For example, Cubizolle et al. (2007) use 30% OM as lower limit for peat in the French Massif Central, whereas for instance Loisel et al. (2013) use 50% OM for an Alaskan peatland. To stimulate the use of quantitative and reproducible definitions, a property such as OM content is recommendable, as it can be measured relatively easily and at low cost. As there is a clear gradient in organic matter (indicated by the variable $M$) at the transition from mineral sediment to peat (i.e., as a function of distance $x$ upwards in the profile), both the mineral-to-peat transition (i.e., the period of peat initiation) and the *basal peat* (i.e., the stratigraphical layer that is defined as the bottom of a peat deposit) can be defined by the organic matter content [$M(x)$] and the organic matter gradient [the derivative given by $\frac{dM}{dx}$] (Fig. 1b).

After defining *basal peat*, adequate sampling and sample pretreatment for radiocarbon dating are required to accurately derive the age of the basal peat layer. The discussion on which samples most

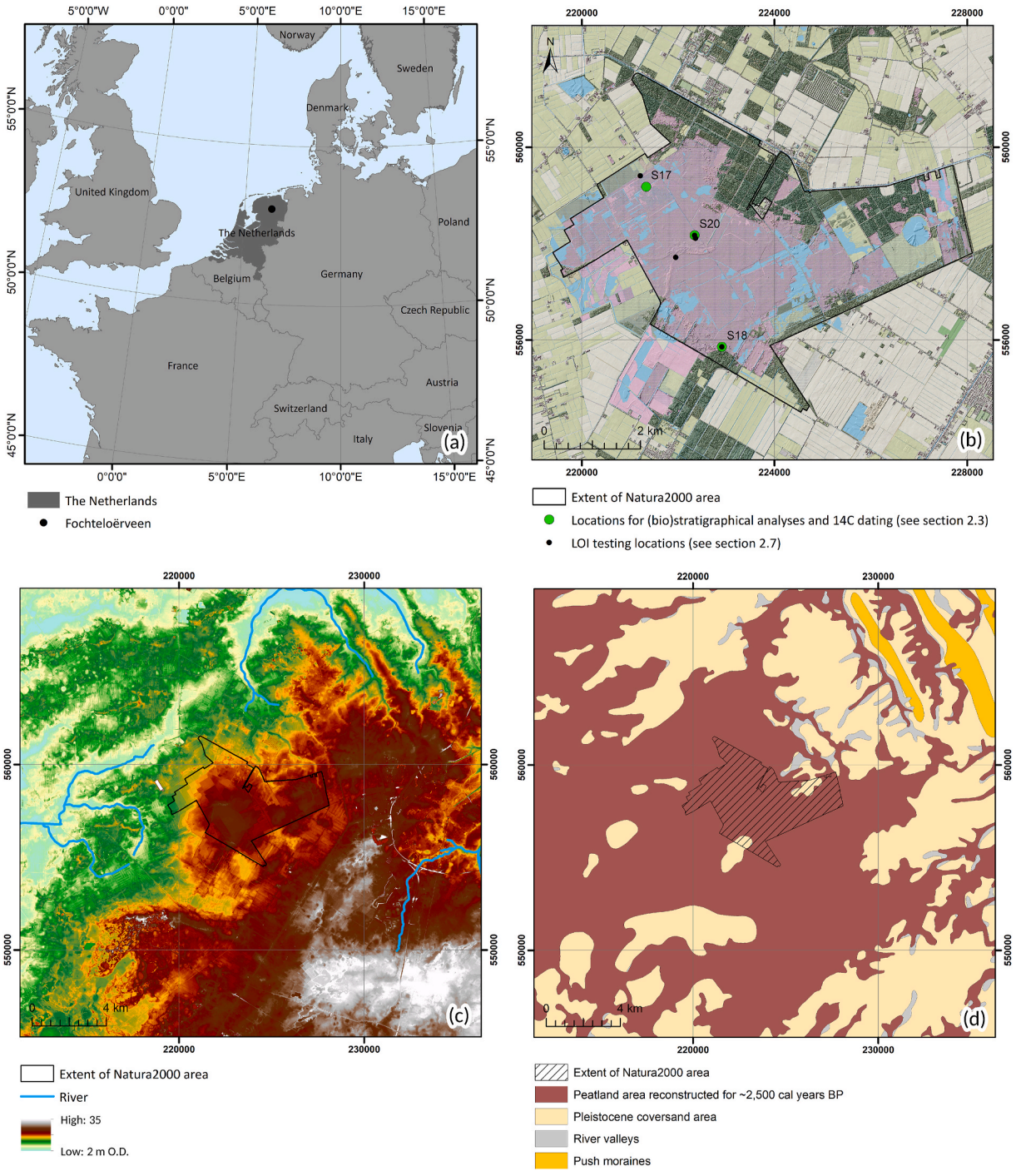


**Fig. 2.** (a) Location of the Netherlands and the Fochteloërveen peat remnant in Europe. (b) Topographical map of Fochteloërveen, indicating sampling locations. Dataframe coordinates are in metres (Dutch RD-new [*Rijksdriehoeksstelsel*] projection). (c) Digital Elevation Model (DEM) of Fochteloërveen and surroundings, showing the main drainage pattern. Elevation is in metres relative to Dutch Ordnance Datum (O.D., roughly mean sea level). (d) Reconstructed palaeogeography for ~2500 cal years BP, indicating assumed former extent of the peatland area around Fochteloërveen. Sources: topography (OpenSimpleTopo, 3200 pixels/km) by Van Aalst (2021); DEM of the Netherlands (AHN3; horizontal resolution 5 m, vertical resolution 0.1 m) from AHN (2021a, 2021b); rivers from Ministerie van Verkeer en Waterstaat (2007); Natura 2000 area from Ministerie van Economische Zaken (2018), palaeogeographical map (500 BC) from Vos and De Vries (2013) and Vos et al. (2020).

accurately indicate the age of peat layers started several decades ago (e.g. Törnqvist et al., 1992, 1998; Shore et al., 1995; Nilsson et al., 2001; Brock et al., 2011; Van der Plicht et al., 2019). Various studies have highlighted multiple concerns with the radiocarbon dating of peat. If carbon from other carbon sources is incorporated or mixed with the original sample material and cannot be removed (by manual selection and/or chemically), this may result in apparent ages that are either too old or too young for the peat layer of interest (Table 1).

Bulk dating is often complicated by difficulties with interpreting the resulting age, which represents a mixture of ages of various organic fractions. The development of AMS in radiocarbon has enabled new possibilities for dating peat deposits due to much lower requirements regarding sample sizes (e.g. Tuniz et al., 1998; Jull and Burr, 2015). The concerns outlined in Table 1 have led to the recommendation to date

short-lived, aboveground plant macrofossils of terrestrial species with AMS (e.g. Piotrowska et al., 2011).

Unfortunately, AMS dating of terrestrial macrofossils is not always possible for mineral-to-peat transitions (Fig. 1c). Depending on the type of mire and local circumstances, the basal peat layer may have an amorphous peat facies largely devoid of (identifiable) plant macrofossils. Limited presence of plant macrofossils may require resorting to bulk sampling for radiocarbon dating the basal peat layer, which could hamper interpretation of dating results. The magnitude of this problem appears to vary. For instance, Törnqvist et al. (1992) found age differences of up to 600 $^{14}$C year between bulk and macrofossil samples from mid-latitude minerotrophic peats, whereas Berendsen et al. (2007), who studied comparable deposits, and Holmquist et al. (2016), who looked at basal peat from circum-arctic peatlands, reported no significant age differences. Depending on the duration of the period in which the basal peat forms, sampling plant macrofossils from higher positions in the peat profile to circumvent bulk sampling at the base may no longer reflect peat initiation, as a potentially large age difference between these layers might exist.

Pre-treatment of bulk samples using acids and base solutions results in multiple organic fractions which are defined based on their solubilities (Brock et al., 2011; Van der Plicht et al., 2019): fulvic acids are soluble in both alkaline and acids, humic acids are soluble in alkaline but insoluble in acids, and humins are insoluble in alkaline and acids. Fulvic acids are usually removed during pre-treatment and not used for dating. Because of their high mobility, which allows them to translocate easily through a soil profile, significantly younger dates might be obtained for fulvics than for the humic and humin fraction from the same layer (Shore et al., 1995). As the solubility of humics is determined by pH and lower under acidic conditions (Wüst et al., 2008), their mobility depends on environmental circumstances and may change through time. There is no clear consensus in literature on whether humic or humin dates are most representative for dating peat layers. Examples range from studies where no significant age differences are reported (e.g. Cook et al., 1998; Waller et al., 2006), studies that consider humins to be most appropriate for peat (e.g. Hammond et al., 1991; Van der Plicht et al., 2019) and humics for deposits with low carbon amounts (Van der Plicht et al., 2019), or where a conclusion that one or the other fraction is more reliable could not be drawn unquestionably (Brock et al., 2011). Moreover, hardly any studies focus on *basal peat* layers while investigating the ages of these organic fractions (with the exception of Brock et al., 2011). It is therefore unknown which carbon fractions of these basal peat layers, which might be slightly different in organic carbon composition (especially in carbon content) compared to peat samples from higher positions in peat profiles, are most representative for the time period of peat initiation.

In the current study we aim to formulate recommendations for dating *basal peat*. Issues that we specifically address are (1) peat initiation is a process of a certain timespan rather than an event, (2) *basal peat* needs to be clearly defined, (3) selection of dating samples is typically challenging due to potential poor preservation of plant macrofossils in *basal peat* and (4) the representativity of humic and humin dates for the age of *basal peat* is questionable. We analyse lithological, biostratigraphical and geochronological characteristics of the mineral-to-peat transition in a bog remnant, focusing on understanding the course of the process of peat initiation and related implications for dating.

## 2. Methods

### 2.1. Selection of study area and overview of methods

The Fochteloërveen peat remnant (the Netherlands, Fig. 2) was selected as case study region. This peatland, with its surface area of approximately 2500 ha, is one of the largest raised bog remnants of Northwest Europe. The area is considered representative for many (non-coastal) peatlands of the Northwest European Plain with regard to the widespread distribution of its mineral substrate and characteristic climatic conditions (see section 2.2). As many European peatlands are subject to ongoing excavation or affected by reclamation relics from historical peat-cutting, basal peat layers may be damaged. In the Fochteloërveen, several former peat cutting pits (some of which are currently artificial lakes) are present and superficial patterns of historical buckwheat fire culture can be recognized. However, the latter disturbed only the surface of the peatland and therefore basal peat layers are undamaged in the majority of the area. A recent study on peat initiation trends in the northern Dutch coversand landscape (Quik et al., 2021) provides background information on peat growth in the wider study region, and demonstrated that the Fochteloërveen (as one of the few surviving bog remnants) has so far received limited scientific attention regarding its initiation and age.

Three sites (named S17, S18 and S20, Fig. 2a and b) in the Fochteloërveen peat remnant were selected for dating (for further details on choices for site selection see section 2.3). At each of these sites a core containing the mineral-to-peat transition was obtained. Note that the meaning of *basal peat* in this study is much broader than the 'Basisveen Bed' as known in Dutch stratigraphy (TNO-GSN, 2021a). For each of the three sites, selected levels in the peat core were analysed for percentage organic matter (OM) through loss-on-ignition (LOI), plant macrofossils (PM) and testate amoebae (TA). The palaeo-environmental setting was reconstructed based on analyses of PM and TA. Based on LOI data, samples for radiocarbon ($^{14}$C) dating were selected from multiple levels within each core. When attainable, (charred) plant macrofossils were selected for dating. Additionally the original bulk material was sampled and chemically processed to derive humic and humin fractions for dating. All steps are explained below.

### 2.2. Study area

The northern Netherlands was covered by a continental ice sheet during the Saalian (MIS 6), which led to deposition of glacial till (Rappol, 1987; Van den Berg and Beets, 1987; Rappol et al., 1989; TNO-GSN, 2021b) on the Drenthe Plateau or till plateau (Ter Wee, 1972; Bosch, 1990). During the Weichselian (OIS 4-2), aeolian coversands were deposited over an extensive area of Northwest Europe, forming the European Sand Belt (Koster, 1988, 2005). On the Drenthe Plateau these coversands occur with a thickness varying from 0.5 to 2 m (Ter Wee, 1979; TNO-GSN, 2021c). The Fochteloërveen peat remnant is located near the western edge of the Drenthe Plateau and is part of three catchments, draining into the rivers Drentsche Aa, Peizerdiep and Tjonger (Fig. 2c). Historical data of the 18th century indicate that peat thickness at the Fochteloërveen has diminished over the past centuries with as much as 7 m at some locations (Douwes and Straathof, 2019). Our corings (see section 2.3) demonstrated that peat thickness currently varies from 20 cm to 225 cm at approximately 100 visited locations distributed over the peatland. Current climate is characterised by average temperatures of 2.8 °C in January and 17.5 °C in July, average annual rainfall of 805 mm, and a potential evapotranspiration of 566 mm (KNMI, 2021).

As a result of large-scale historical peatland reclamations (e.g. Gerding, 1995; Van Beek et al., 2015) currently only small remnants of the former extensive Northwest European peat landscapes remain (Fig. 2d). The Fochteloërveen remnant is protected as Natura 2000 area and harbours a wide range of plant and animal species (Provincie Drenthe, 2016). Main threats to the quality and continuity of the area include atmospheric nitrogen deposition and desiccation due to intense drainage for surrounding agriculture. Since the 1980s nature conservation is aimed at peatland restoration (Straathof et al., 2017).

### 2.3. Site selection and stratigraphy

We performed an elaborate field exploration of the peat remnant consisting of around 100 corings (some grouped in transects of 185–575

**Table 2**
Lithology and lithogenetic interpretation of the stratigraphical layers occurring from the surface downwards (modified from Bos et al., 2012).

| Lithology | Symbol | Lithogenetic interpretation |
|---|---|---|
| Peat with brown colouring and clearly recognisable plant remains. | V3 | Non-decomposed peat |
| Peat with blackish-brown colouring, greasy consistency and very few recognisable plant remains. | V3* | Amorphous peat (highly humified; *sapric* cf. WRB-IUSS, 2015) |
| Mixture of peat with very fine to moderately fine sand, dark brown colouring. | ZV/VZ | Peaty sand/sandy peat (gradual transition zone from Pleistocene mineral deposits to overlying organic deposits) |
| Very fine to moderately fine sand with colour varying from dark brown to light grey, locally loamy, sporadically containing pebbles (ø 1–5 mm). | P | Pleistocene mineral deposits |

m long). For each core the stratigraphy was described (see Table 2 for details).

As the basal peat is not oligotrophic (see Results for further information), field determination of the degree of humification using the scale for ombrotrophic peat by Von Post (Aaby, 1986) does not fully apply. Additionally, the use of Munsell colour charts for fresh organic deposits is often difficult as the material changes in colour following exposure to oxygen. Instead, we applied a simplified version of the organic-facies determination key by Bos et al. (2012), which is originally intended for organic sediments in deltaic settings. Our basic field classification differentiates amorphous organic material (similar to *amorphous organics* in Bos et al., 2012), and non-decomposed peat (similar to *oligotrophic peat* in Bos et al., 2012) where further botanical specification is obtained later through microscopic analyses of plant macrofossils.

Following the field exploration, 21 cores originating from sites distributed over the peatland were collected for future analyses. To address the current research aim, three cores were selected based on a set of criteria considering lithological representativity, spatial distribution and elevation (see Table 3 for a comparison of these properties and further details on selection criteria). Each core was collected from a transect along a coversand ridge that underlies the peat deposits. Site S17 (transect in Fig. 3) is located in what is probably a valley or topographic low in the sand landscape underlying the peat deposits, cores S20 and S18 (transects not shown) are located at peat-covered flanks of sand ridges.

### 2.4. Collection of cores

The three cores were collected in 2019 with a hand-operated stainless-steel peat corer (Russian type) of 50 cm long and 60 mm outer diameter, with an equivalent core volume of 0.5 $dm^3$ (Eijkelkamp Soil and Water, 2018). This type of corer was found to be most useful for sampling both peat and water saturated mineral sediments underneath in one core, with minimal disturbance and low risk of contamination. Other types of corers were considered unsuitable for this purpose. For instance, augers or gouge corers often disturb the sample and do not protect it from contamination as there is no closed coring chamber. A Van der Staay suction corer (Wallinga and Van der Staay, 1999), which is used to sample water saturated mineral deposits, cannot sample peat layers as these block the suction mechanism. The Russian corer is generally used for sampling deeper (i.e. mostly catotelm) peat layers (De Vleeschouwer et al., 2010). Field testing demonstrated that this corer was able to simultaneously sample both peat and the top of water saturated mineral deposits adequately (Fig. 4). In areas where the

**Table 3**
(a) Criteria for the selection of sites for a vertical dating series, with their respective rationale. (b) Properties of the three sampled sites compared with the minimum (Min), maximum (Max) and average (Avg) of the in total 21 sampled sites of the peat remnant (i.e., where a core for analyses was collected). The surface elevation was measured with a vertical precision of ~10 mm. The total thickness of organic deposits is the sum of V3, V3* and ZV/VZ. The top of the Pleistocene mineral deposits was derived from the surface elevation minus the total thickness of organic deposits as determined visually in the field (i.e., might deviate slightly from the basal peat layer that was defined later based on OM%). NA = not applicable. For other stratigraphical abbreviations see explanation in Table 2.

(a)

| Selection criteria | Rationale |
|---|---|
| The site is part of a coring transect (distance between 185 and 575 m long). | The coring transect provides relevant background information regarding the landscape position of the site. |
| The obtained core contains the (visual) mineral-to-peat transition. | Cores containing the mineral-to-peat transition will be most straightforward to analyse and are not compromised by suboptimal sampling conditions. |
| For the three selected sites, the cores have V3* layers of varying thickness, and at least one site contains a ZV layer. | Analyses of three sites with a representative thickness range of V3* and presence of a ZV layer will cover the stratigraphical diversity that is present in the study area (see Table 3b) and potentially in other regions. This ensures that any methodological recommendations will have a wide applicability. |
| The three selected sample sites are well-distributed spatially and of varying elevation. | Our approach should be applicable to different landscape positions. |

(b)

| Property | S17 | S18 | S20 | Min | Max | Avg |
|---|---|---|---|---|---|---|
| Surface elevation (m O.D.) | 9.308 | 11.999 | 10.781 | 9.31 | 12.00 | 10.70 |
| Total thickness organic deposits (cm) | 216 | 30 | 35 | 30 | 216 | 94 |
| Thickness V3 (cm) | 182 | 16 | 24 | 16 | 182 | 74 |
| Thickness V3* (cm) | 34 | 6 | 11 | 6 | 34 | 17 |
| Thickness ZV/VZ (cm) | 0 | 8 | 0 | 0 | 8 | 3 |
| Top of Pleistocene mineral deposits (m O.D.) | 7.15 | 11.70 | 10.26[a] | 7.15 | 11.70 | 9.70 |
| Location | East | West | Central | NA | NA | NA |

[a] Corrected for standing water at the surface.

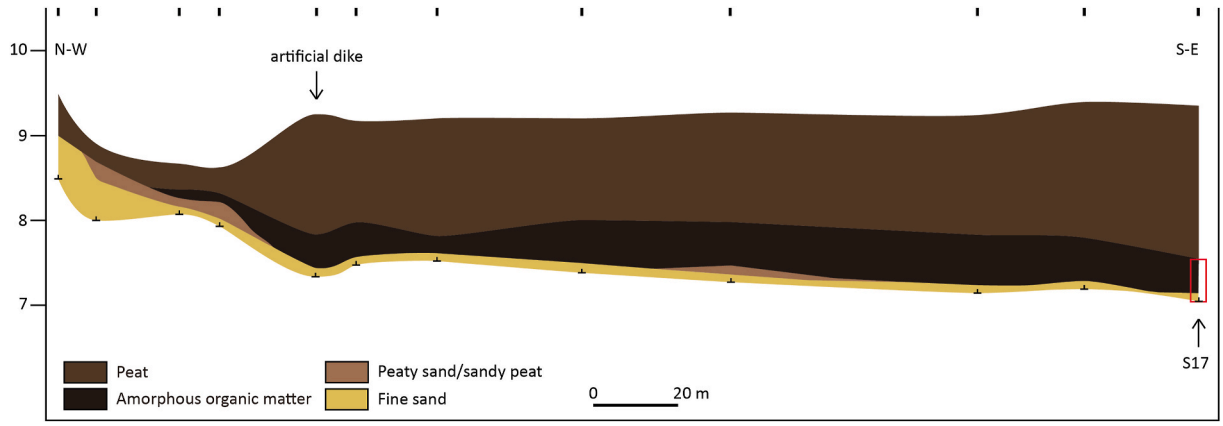


**Fig. 3.** Example cross section, showing stratigraphical context of core S17 (on the right). The red box indicates the sampled reach of the profile. About 1 m further in S-E direction, a wide ditch hampered additional corings to extend the transect.

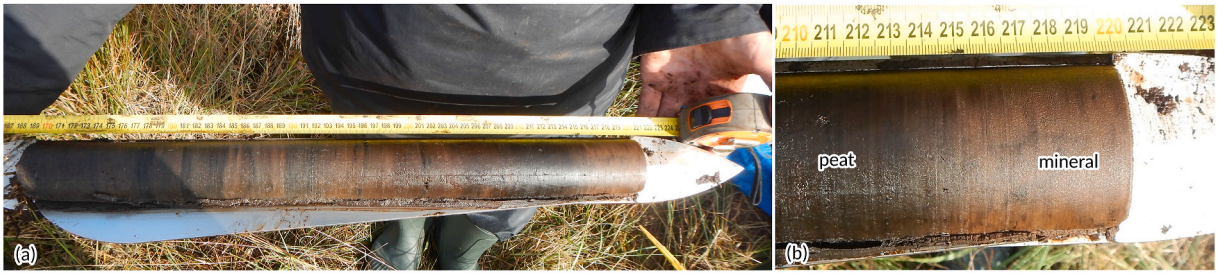


**Fig. 4.** Photograph of core S17 taken directly after collecting the core in the field, (a) overview photo (bottom at the right), (b) detail of the mineral-to-peat transition.

mineral deposits are compacted so firmly that hand-operated corers cannot be pressed down to a sufficient depth, the use of percussion drilling equipment might be useful (e.g. Eijkelkamp Agrisearch Equipment, 2022).

Each time prior to sampling a new core, the coring chamber and pivoting blade (fin or lid) were cleaned with a fresh microfiber cloth, followed by a thorough rinse with deionised water. Directly after this cleansing routine the corer was pressed down with the pivoting blade closed. After reaching the desired sampling depth the corer was turned 180° clockwise to collect the sample, upon which the pivoting blade closed the coring chamber and the corer was retrieved. Subsequently the corer was kept horizontally with the pivoting blade facing upwards. The blade was carefully turned to retrieve the (undisturbed) core. At this point the core was photographed. Retrieval and packaging of the core followed the procedures proposed by De Vleeschouwer et al. (2010) and Givelet et al. (2004), and proceeded as follows. The core was covered with plastic cling film. Then a PVC half-circular pipe was placed over the core, upon which the corer was rotated to transfer the plastic-covered core to the PVC pipe. The exposed side was covered with the remaining plastic film and the core was secured with plastic tape. Through these steps, which took about 5 min from retrieval to packaging, handling of the core in the field was minimized. The name, top and bottom of the core were marked with water-resistant labels. The PVC pipes were transported in horizontal orientation to prevent damage to the cores and stored in a refrigerator of 3 °C within 12 h. Location and elevation of all sampling sites were recorded with a Topcon 250 Global Navigation Satellite System (GNSS) receiver, with a horizontal precision of ~5 mm and vertical precision of ~10 mm (RTK; TOPCON, 2017).

### 2.5. Core processing and subsampling

The cores were opened in the laboratory of BIAX Consult (Zaandam, the Netherlands). Each core was photographed again, the stratigraphy was described and based on visual inspection the approximate mineral-to-peat transition was determined. Around this transition, a range of contiguous 1-cm-thick slices was cut from the core. Outer edges of each slice were carefully cleaned to prevent contamination. Total sample volume for each cleaned level amounted to ~7 $cm^3$. The samples were subsampled for multi-proxy analysis based on a priority flowchart (Fig. 5), which is further explained below.

A bulk subsample (2 $cm^3$) was collected for dating. The remaining material (around 5 $cm^3$) was used for PM to analyse plant species and to select suitable plant macrofossils for radiocarbon dating. The PM subsamples were obtained from the filtrate after gently rinsing with warm water over a 0.25 mm sieve. A pollen sample (0.5 ml) was collected from the sieving water for future study and stored at 3 °C. Sieving water (0.5 ml) and any remaining non-sieved material (ranging between 1 up to 3 $cm^3$ depending on how much material remained) was collected for TA analysis. Considering its destructive protocol, LOI was performed only on non-sieved material that remained after TA analysis (typically between 1 and 2 $cm^3$). To gain more insight in the organic matter gradient in the cores, additional levels were sampled where only LOI was performed (without biostratigraphical analyses and $^{14}C$ dating). For these levels 2 $cm^3$ of unsieved material was used for LOI, the remainder was stored at 3 °C for future reference. Table 4 provides an overview of all collected subsamples for the three cores.

### 2.6. (Bio)stratigraphical analyses

The percentage organic matter was determined using LOI (see e.g. Chambers et al., 2011; Kennedy and Woods, 2013). The used subsamples for LOI had a volume of 1–2 $cm^3$. Sample dry weight was determined after drying for 24 h at 105 °C, followed by combustion at 550 °C. Subsample dry weight was ~0.65 g on average, of which the remaining

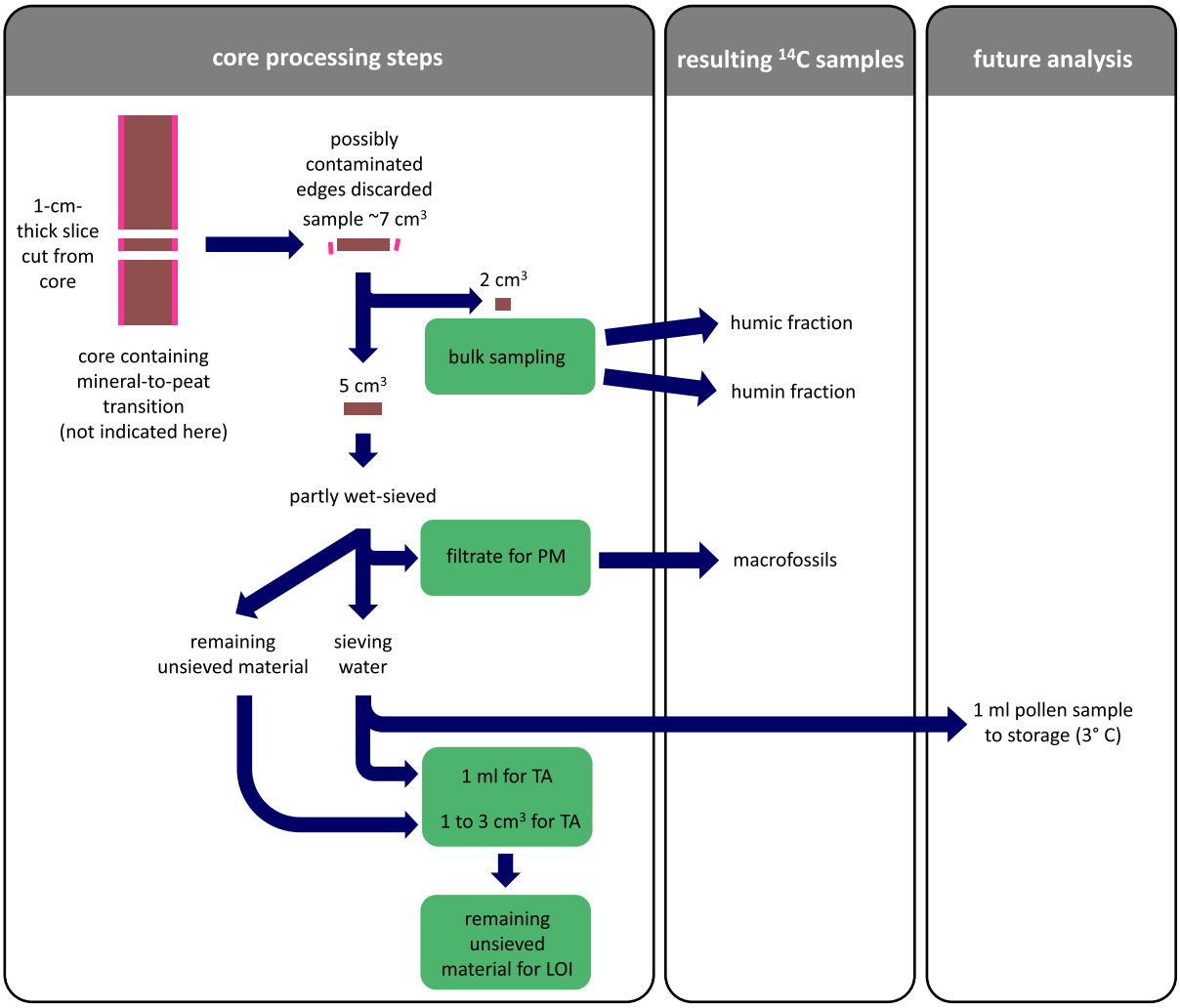


**Fig. 5.** Flowchart showing allocation of sample material from each 1-cm-thick core slice, subsequent processing steps and resulting fractions for $^{14}$C dating. PM = plant macrofossil analysis, TA = testate amoebae analysis, LOI = loss-on-ignition.

mineral component (dry ash) after combustion amounted to ~0.29 g. A microbalance (0.0001 g) was used to maximise measurement precision for these small subsample sizes.

PM analyses were conducted at BIAX Consult in Zaandam, the Netherlands. Mosses and seed remains of vascular plants in the filtrate were identified with a Leica binocular incident light microscope at magnifications of x6 to x50. Identifications followed Körber-Grohne (1964, 1991), Berggren (1969, 1981), Anderberg (1994), Smith (2004), and Cappers et al. (2006).

TA subsamples were analysed at Queen's University Belfast, United Kingdom. These subsamples were wet-sieved at 300 μm and back-sieved at 15 μm following standard procedures described by Booth et al. (2010). Two slides per sample (2 × 21 × 21 mm cover glasses) were studied using a high power binocular microscope under x20 to x40 magnification.

### 2.7. Defining basal peat (determining $M_d$ value)

To gain a thorough understanding of the OM gradient around the mineral-to-peat transition in our study area prior to selecting a defining OM value (i.e., $M_d$, Fig. 1b) above which the material is called *peat*, a vertical series of LOI measurements was performed for five duplicate cores (i.e., additional cores that were collected approximately 10 cm next to the locations of the 21 sampling sites). In this way, the OM gradient could be determined for a continuous sequence (of 22–26 cm long) with a resolution of 1 cm (note that this was not fully possible for the cores of sites S17, S18 and S20 that were collected for dating, as for some investigated levels no unsieved material remained after completion of the biostratigraphical analyses to perform LOI). The resulting OM gradients were analysed to derive a substantiated value for $M_d$.

### 2.8. Radiocarbon dating

The material reserved for bulk sampling was used without removal of roots and provided sufficient humics and humins to date for nearly each level (Table 4). For plant macrofossil samples, only charred aboveground plant material was selected for radiocarbon dating; waterlogged (uncharred) belowground plant remains like rootlets, radicelles and rhizomes were present abundantly, but aboveground waterlogged plant remains were scarce. From 22 levels of the three cores, charred aboveground plant remains from terrestrial plants could be retrieved (Tables 4 and 5).

Radiocarbon measurements were performed at the Centre for Isotope Research of the University of Groningen (the Netherlands), using a MICADAS Accelerator Mass Spectrometer (Ionplus AG; Synal et al., 2007). For background information on the principles of radiocarbon dating we refer to e.g. Bayliss et al. (2004); Bronk Ramsey (2008a); and Törnqvist et al. (2015). For a full description of the (pre-treatment) methods in Groningen we refer to Dee et al. (2020). Here we only concisely describe details of chemical pre-treatment and other relevant

**Table 4**
Overview of analyses and resulting fractions for $^{14}C$ dating for each investigated level of the cores S17, S18 and S20. PM = plant macrofossil, TA = testate amoebae, LOI = loss-on-ignition.

| Core | From (m O.D.) | To (m O.D.) | PM analysis | TA analysis | LOI | $^{14}C$ bulk humic | $^{14}C$ bulk humin | $^{14}C$ macrofossils |
|---|---|---|---|---|---|---|---|---|
| S17 | 7.495 | 7.505 | X | X | | X | X | X |
| | 7.485 | 7.495 | X | X | X | X | X | X |
| | 7.475 | 7.485 | X | X | | X | X | X |
| | 7.430 | 7.440 | X | | X | | | |
| | 7.390 | 7.400 | X | | X | | | |
| | 7.350 | 7.360 | | | X | | | |
| | 7.300 | 7.310 | X | X | X | X | X | X |
| | 7.290 | 7.300 | X | X | X | X | X | X |
| | 7.280 | 7.290 | X | X | | X | X | X |
| | 7.230 | 7.240 | | | X | | | |
| | 7.220 | 7.230 | | | X | | | |
| | 7.210 | 7.220 | X | X | X | X | X | X |
| | 7.200 | 7.210 | X | X | X | X | X | X |
| | 7.190 | 7.200 | X | X | | X | X | X |
| | 7.180 | 7.190 | X | X | X | | X | |
| | 7.170 | 7.180 | X | X | X | X | X | |
| S18 | 11.80 | 11.81 | X | X | X | X | X | |
| | 11.79 | 11.80 | X | X | X | X | X | X |
| | 11.78 | 11.79 | X | X | X | X | X | X |
| | 11.77 | 11.78 | X | X | | X | X | X |
| | 11.76 | 11.77 | | | X | | | |
| | 11.75 | 11.76 | | | X | | | |
| | 11.74 | 11.75 | | | X | | | |
| | 11.73 | 11.74 | X | X | | X | X | X |
| | 11.72 | 11.73 | X | X | X | X | X | X |
| | 11.71 | 11.72 | X | X | X | X | X | |
| | 11.70 | 11.71 | X | X | | X | X | |
| | 11.69 | 11.70 | | | X | | | |
| | 11.68 | 11.69 | X | X | | X | X | |
| | 11.67 | 11.68 | X | X | X | X | X | |
| | 11.66 | 11.67 | X | X | X | X | X | |
| | 11.65 | 11.66 | X | X | | X | X | |
| S20 | 10.40 | 10.41 | | | X | | | |
| | 10.39 | 10.40 | | | X | | | |
| | 10.38 | 10.39 | X | X | X | X | X | |
| | 10.37 | 10.38 | X | X | X | X | X | X |
| | 10.36 | 10.37 | X | X | X | X | X | X |
| | 10.35 | 10.36 | X | X | X | | X | |
| | 10.34 | 10.35 | | | X | | | |
| | 10.33 | 10.34 | X | X | X | X | X | X |
| | 10.32 | 10.33 | X | X | X | X | X | X |
| | 10.31 | 10.32 | X | X | | X | X | X |
| | 10.30 | 10.31 | X | X | X | X | X | |
| | 10.29 | 10.30 | X | X | | X | X | |
| | 10.28 | 10.29 | | | X | | | |
| | 10.27 | 10.28 | | | X | | | |
| | 10.26 | 10.27 | X | X | | X | X | X |
| | 10.25 | 10.26 | X | X | X | X | X | X |
| | 10.24 | 10.25 | X | X | X | X | X | X |

characteristics of our dating samples.

The acid-base-acid (ABA) method was applied to all the charred plant remains, with respective temperatures of 80°, 80° and 20 °C. For the humin and humic fractions the bulk sample material was first pre-treated with acid and base, both at 80 °C. Then the base solution was kept separate and the humic fraction was obtained by addition of acid (at 20 °C). The solid humic fraction was rinsed with decarbonized water to almost neutral pH and dried in an oven at 80 °C. The solid material (humin fraction) that remained after the base step was rinsed to neutral pH and then treated with acid (at 20 °C), rinsed with decarbonized water to neutral pH and dried in an oven at 80 °C. The sample material was not sieved during the entire procedure, to secure that the very small organic particles in the bulk material were retained. Instead, a centrifuge was used to separate the solid and liquid fractions. Some of the humin fraction samples contained a lot of sand and little organic remains, which resulted in a very low carbon yield of the combusted subsample (Tables 7–9). Also the obtained humic fraction yields were very low for several samples.

After chemical pre-treatment (sub)samples were weighed in tin capsules and combusted to $CO_2$ in an elemental analyser (IsotubeCube NCS). This analyser is coupled to an Isotope Ratio Mass Spectrometer (Isoprime 100) for measurement of $\delta^{13}C$ in the sample material. Resultant $CO_2$ was graphitized to carbon using hydrogen and an iron catalyst. The graphite was pressed into aluminium cathodes and measured on $^{12}C$, $^{13}C$ and $^{14}C$ atoms with the MICADAS. The samples measured as graphite in the AMS, can be divided in two groups. Part of the humic and humin fractions were relatively small (up to 1 mg carbon) and these samples were measured in an AMS batch for small-sized samples. The measurement error for these samples is around ±40 yrBP. The other part of the samples was measured as graphite in a regular AMS batch (for masses >1 mg and <2.5 mg C) and the measurement uncertainty for these samples is in general below ±30 yrBP.

Three charred plant remains samples of S17 (M6, M12 and M3) and one humic fraction of S18 (M12) had very small sizes (<0.5 mg) and were treated in a different way. These samples were combusted with an elemental analyser (Isotube Cube) to $CO_2$. The $CO_2$ was led into the AMS

**Table 5**
Overview of the charred aboveground plant remains that were selected for radiocarbon dating. When a number is given, this is the exact amount encountered, cf. = resembles, + = present, ++ = frequent. The sample weight is the mass of the sample before the start of the chemical pre-treatment.

| Core | From (m O.D.) | To (m O.D.) | Aboveground plant remains (all charred) for $^{14}$C dating | Sample weight (mg) |
|---|---|---|---|---|
| S17 | 7.495 | 7.505 | *Calluna vulgaris*, twig fragments +<br>Herbaceous stem, fragments +<br>*Sphagnum*, stem fragments + | 8.63 |
| | 7.485 | 7.495 | *Erica tetralix*, leaf fragments +<br>*Calluna vulgaris*, twig fragments +<br>*Calluna/Erica*, twig fragments +<br>Herbaceous stem, fragments +<br>*Bryales*, stem fragments + | 20.78 |
| | 7.475 | 7.485 | *Erica tetralix*, 3 leaves<br>*Eriophorum vaginatum*, 1 spindle<br>*Calluna/Erica*, twig fragments + | 4.21 |
| | 7.300 | 7.310 | Deciduous wood, undetermined | 1.36 |
| | 7.290 | 7.300 | Herbaceous stem fragments + | 0.87 |
| | 7.280 | 7.290 | Herbaceous stem ~18 fragments (incl. cf. *Juncus*) | 11.75 |
| | 7.210 | 7.220 | Herbaceous stem fragments (cf. *Eriophorum*) ++ | 9.70 |
| | 7.200 | 7.210 | Herbaceous stem and stem base fragments (cf. *Eriophorum*) ++ | 12.99 |
| | 7.190 | 7.200 | Herbaceous stem ~16 small fragments | 3.07 |
| S18 | 11.79 | 11.80 | *Calluna vulgaris*, twig fragments +<br>*Calluna/Erica*, twig fragments +<br>Herbaceous stem, fragments +<br>*Sphagnum*, stem fragments + | 2.34 |
| | 11.78 | 11.79 | *Calluna/Erica*, twig fragments +<br>Herbaceous stem, fragments + | 0.57 |
| | 11.77 | 11.78 | Cyperaceae (cf. *Eriophorum*), stem base 3 fragments<br>Herbaceous stem, fragments + | 3.30 |
| | 11.73 | 11.74 | *Calluna/Erica*, twig fragments (lower parts) +<br>Herbaceous stem, fragments +<br>*Sphagnum*, stem 1 fragment | 8.16 |
| | 11.72 | 11.73 | *Calluna/Erica*, twig fragments +<br>Herbaceous stem, fragments + | 7.44 |
| S20 | 10.37 | 10.38 | *Erica tetralix*, 1 leaf<br>*Calluna/Erica*, twig fragments + | 4.98 |
| | 10.36 | 10.37 | *Erica tetralix*, 2 leaves<br>*Calluna/Erica*, twig fragments + | 18.09 |
| | 10.33 | 10.34 | *Erica tetralix*, 1 leaf<br>*Calluna/Erica*, twig fragments +<br>*Bryales*, stem fragments + | 4.86 |
| | 10.32 | 10.33 | *Calluna/Erica*, twig fragments | 5.26 |
| | 10.31 | 10.32 | *Calluna/Erica*, twig fragments +<br>Herbaceous stem, fragments + | 4.47 |
| | 10.26 | 10.27 | Herbaceous stem, 2 small fragments | 0.04 |
| | 10.25 | 10.26 | Herbaceous stem, fragments +<br>Charcoal, small fragments + | 1.58 |
| | 10.24 | 10.25 | Herbaceous stem, 1 fragment<br>Charcoal, 1 small fragment | 1.04 |

and measured directly on carbon isotopes. Since much lower carbon masses are measured in the AMS (in a much shorter time period) when introduced as $CO_2$ gas compared to graphite samples, the measurement uncertainty for these samples is larger (±60–80 yrBP) compared to the samples measured as graphite.

The $^{14}$C measurement results ($F^{14}C$ and $^{14}$C age in Tables 7–9) are calculated according to the conventions (Stuiver and Polach, 1977), OX-II (SRM 4990C) was used as calibration standard, and the results are corrected for background signals using background reference materials and for isotopic fractionation using the $\delta^{13}C$ value measured with AMS.

### 2.9. Calibration and age-depth modelling

The radiocarbon dates were calibrated using IntCal20 (Reimer et al., 2020) in the OxCal program (version 4.4, Bronk Ramsey, 1995). The calibrated ages are presented as likelihoods in age-depth plots in OxCal (i.e., initially no further assumptions were applied in a Bayesian modelling framework). Subsequent modelling was based on the following assumptions:

- Plant macrofossil ages provide the best estimate of the age of a peat layer (based on correct chronology as shown in Fig. 7a/e/i and in line with the consensus in literature to date short-lived, aboveground plant macrofossils of terrestrial species with AMS, see e.g. Piotrowska et al., 2011).
- For reasons outlined in Fig. 1, humic and humin samples may potentially yield different ages than plant macrofossil samples.
- Agreement of humic/humin ages with plant macrofossil ages indicates that the humic/humin samples are contemporaneous with the peat layer from which they were obtained. As such, they provide a representative indication of the age of the peat layer.
- In contrast, disagreement of humic/humin ages with plant macrofossil ages indicates that the humic/humin samples are not contemporaneous with the peat layer from which they were obtained, and do not accurately represent the age of the peat layer.

For each core, the dates of plant macrofossils were modelled using the P_Sequence function (Bronk Ramsey, 2008b) as follows. Start and end of the P_Sequence were defined with a Tau_Boundary and regular Boundary respectively. The levels of the start of the peat initiation

**Table 6**
Results of the analyses of plant macrofossils and testate amoebae. When a number is given, this is the exact amount encountered, (c) = charred, cf. = resembles, + = present, ++ = frequent, +++ = abundant, ++++ = extremely abundant, NA = not available. Final column indicates stratigraphy (also see Table 2), MtP (indicated with light grey shading) = mineral-to-peat transition (see Fig. 7), BP = basal peat.

| Core | From (m O.D.) | To (m O.D.) | *Sphagnum*, stem fragments (c) | *Sphagnum austinii*, leaves | *Bryales*, stems (c) | *Calluna vulgaris*, twig fragments (c) | *Calluna vulgaris*, leaves (c) | *Calluna vulgaris*, leaves | *Calluna/Erica*, twig fragments (c) | *Erica tetralix*, leaves, fragments (c) | *Erica tetralix*, leaves, fragments | Poaceae (excl. *Phragmites*), leaf/stem epidermis | Poaceae (incl. *Phragmites*), leaf/stem epidermis | *Eriophorum vaginatum*, spindle (c) | Cyperaceae, cf. *Eriophorum*, stem base (c) | Herbaceous stem fragments (c) | *Juncus*, seeds | *Juncus conglomeratus/effusus*, seeds | *Carex*, radicelle | Cyperaceae, rootlets/radicelle | Undetermined rootlets/radicelle | Undetermined rhizome epidermis | Wood, decidous, fragments (c) | *Cenococcum geophilum*, sclerotia | *Selaginella selaginoides*, megaspores | *Difflugia* | *Difflugia pristis* | Charcoal, fragments | Fine sand | Stratigraphy |
|---|---|---|---|---|---|---|---|---|---|---|---|---|---|---|---|---|---|---|---|---|---|---|---|---|---|---|---|---|---|---|
| 17 | 7.495 | 7.505 | + | + | | + | | | | | | | | | | + | | | | | +++ | + | | | | | | | | peat |
| 17 | 7.485 | 7.495 | | + | + | + | | 2 | + | + | | | | | | + | | | | | + | + | | | | | | | | peat |
| 17 | 7.475 | 7.485 | | | | | | | + | 3 | | | | 1 | | | | | | | +++ | | | | | | | | | peat |
| | \|\| | \|\| | | | | | | | | | | | | | | | | | | | | | | | | | | | | |
| 17 | 7.430 | 7.440 | | | | 8 | 2 | | | 12 | 1 | | | | | | | | | | | | | | | NA | NA | | | peat |
| | \|\| | \|\| | | | | | | | | | | | | | | | | | | | | | | | | | | | | |
| 17 | 7.390 | 7.400 | | | + | | | | | | | | | | | + | + | | | | | | | + | | NA | NA | | | peat |
| | \|\| | \|\| | | | | | | | | | | | | | | | | | | | | | | | | | | | | |
| 17 | 7.300 | 7.310 | | | | | | | | | | | | | | | | | | + | + | ++ | + | ++++ | | | | | | peat |
| 17 | 7.290 | 7.300 | | | | | | | | | | | | | | + | | | | + | +++ | +++ | | +++ | | | | | | peat |
| 17 | 7.280 | 7.290 | | | | | | | | | | | | | | 18 | | | | | | + | | ++ | | | | | | peat |
| | \|\| | \|\| | | | | | | | | | | | | | | | | | | | | | | | | | | | | |
| 17 | 7.210 | 7.220 | | | | | | | | | | | | | + | ++ | | | + | + | + | + | | | | | | | | MtP |
| 17 | 7.200 | 7.210 | | | | | | | | | | | | | + | ++ | | | + | + | + | + | | | | | | | | BP |
| 17 | 7.190 | 7.200 | | + | | | | | | | | | | | | 16 | | | + | + | + | + | | | | | | | | MtP |
| 17 | 7.180 | 7.190 | | | | | | | | | | | | | | | | | + | + | + | + | | | | | | | | MtP |
| 17 | 7.170 | 7.180 | | + | | | | | | | | | | | | | | | + | + | + | | | | | 6 | | 2 | | MtP |
| 18 | 11.79 | 11.80 | + | | | + | | | + | | | | | | | + | | ++ | + | + | + | | | | | | | | | peat |
| 18 | 11.78 | 11.79 | | | | | | | + | | | | | | | + | | ++ | + | + | + | | | | | | | | | MtP |
| 18 | 11.77 | 11.78 | | | | | | | | | | | | | 3 | + | | ++ | + | + | + | | | | | | | | | MtP |
| | \|\| | \|\| | | | | | | | | | | | | | | | | | | | | | | | | | | | | |
| 18 | 11.73 | 11.74 | + | | | | | | + | | | | | | | + | | | + | + | + | | | | | 1 | | | | BP |
| 18 | 11.72 | 11.73 | | | | | | | + | | | | | | | + | | | + | + | + | | | | | | | | + | MtP |
| 18 | 11.71 | 11.72 | | | | | | | | | | | | | | | | | + | + | + | | | | | | | | + | mineral |
| 18 | 11.70 | 11.71 | | | | | | | | | | | | | | | | | + | ++ | ++ | | | + | | | | | + | mineral |
| | \|\| | \|\| | | | | | | | | | | | | | | | | | | | | | | | | | | | | |
| 18 | 11.68 | 11.69 | | | | | | | | | | | | | | | | | + | ++ | ++ | | | + | | | | | | mineral |
| 18 | 11.67 | 11.68 | | | | | | | | | | | | | | | | | + | + | + | | | | | | | | +++ | mineral |
| 18 | 11.66 | 11.67 | | | | | | | | | | | | | | | | | + | + | + | | | | | | | | +++ | mineral |
| 18 | 11.65 | 11.66 | | | | | | | | | | | | | | | | | + | ++ | ++ | | | + | | | | | +++ | mineral |
| 20 | 10.37 | 10.38 | | | | | | | + | 1 | | | | | | | | ++ | | ++ | + | | | | | | | | | peat |
| 20 | 10.36 | 10.37 | | | | | | | + | 2 | | | | | | | | | + | + | ++ | | | | | | | | | peat |
| | \|\| | \|\| | | | | | | | | | | | | | | | | | | | | | | | | | | | | |
| 20 | 10.33 | 10.34 | | | + | | | | + | 1 | | | + | | | | | | | + | ++ | + | | | | | | | | MtP |
| 20 | 10.32 | 10.33 | | | | | | | + | | | | | | | | | | | + | ++ | + | | | | | | | | MtP |
| 20 | 10.31 | 10.32 | | | | | | | + | | | | | | | + | | | | + | ++ | + | | | | | | | | MtP |
| 20 | 10.30 | 10.31 | | | | | | | | | | + | | | | | | | + | + | ++ | | | | | | | | | BP |
| 20 | 10.29 | 10.30 | | | | | | | | | | | | | | | | | | + | ++ | | | | | 1 | | | | MtP |
| | \|\| | \|\| | | | | | | | | | | | | | | | | | | | | | | | | | | | | |
| 20 | 10.26 | 10.27 | | | | | | | | | | | | | | 2 | | | + | + | ++ | | | | | | | | ++ | mineral |
| 20 | 10.25 | 10.26 | | | | | | | | | | | | | | + | | | | + | ++ | | | ++ | | | | + | ++ | mineral |
| 20 | 10.24 | 10.25 | | | | | | | | | | | | | | 1 | | | + | + | ++ | | | | | | | 1 | ++ | mineral |

**Table 7**
Dating results for core S17. CPR = charred plant remains, NA = not available.

| From (m O.D.) | To (m O.D.) | Sample name | Dated fraction | Lab-ID | $F^{14}C$ | ± (1σ) | $^{14}C$ age (yrBP) | ± (1σ) | $\delta^{13}C$ (IRMS) | ± (1σ) | %C |
|---|---|---|---|---|---|---|---|---|---|---|---|
| 7.495 | 7.505 | S17-M9-B | humin | GrM-23376 | 0.5775 | 0.0019 | 4410 | 26 | −27.09 | 0.15 | 62.1 |
| 7.485 | 7.495 | S17-M8-B | humin | GrM-23797 | 0.5759 | 0.0018 | 4433 | 26 | −27.17 | 0.15 | 55.0 |
| 7.475 | 7.485 | S17-M7-B | humin | GrM-23515 | 0.5354 | 0.0017 | 5019 | 26 | −27.62 | 0.15 | 64.5 |
| 7.300 | 7.310 | S17-M6-B | humin | GrM-23516 | 0.4345 | 0.0015 | 6696 | 29 | −27.56 | 0.15 | 63.7 |
| 7.290 | 7.300 | S17-M5-B | humin | GrM-23517 | 0.4504 | 0.0016 | 6407 | 29 | −28.57 | 0.15 | 55.5 |
| 7.280 | 7.290 | S17-M4-B | humin | GrM-23520 | 0.4255 | 0.0016 | 6864 | 30 | −27.79 | 0.15 | 56.3 |
| 7.210 | 7.220 | S17-M12-B | humin | GrM-23731 | 0.4973 | 0.0017 | 5612 | 27 | −28.28 | 0.15 | 13.9 |
| 7.200 | 7.210 | S17-M11-B | humin | GrM-23732 | 0.4817 | 0.0017 | 5868 | 29 | −28.08 | 0.15 | 5.9 |
| 7.190 | 7.200 | S17-M3-B | humin | GrM-23733 | 0.4247 | 0.0016 | 6878 | 30 | −28.25 | 0.15 | 9.5 |
| 7.180 | 7.190 | S17-M2-B | humin | GrM-23734 | 0.4644 | 0.0017 | 6162 | 29 | −28.05 | 0.15 | 10.7 |
| 7.170 | 7.180 | S17-M1-B | humin | GrM-23736 | 0.5023 | 0.0017 | 5532 | 27 | −28.16 | 0.15 | 7.2 |
| 7.495 | 7.505 | S17-M9-B | humic | GrM-23285 | 0.5821 | 0.0019 | 4346 | 26 | −28.13 | 0.15 | 57.2 |
| 7.485 | 7.495 | S17-M8-B | humic | GrM-23829 | 0.5759 | 0.0019 | 4433 | 27 | −27.09 | 0.15 | 50.5 |
| 7.475 | 7.485 | S17-M7-B | humic | GrM-23830 | 0.5477 | 0.0018 | 4836 | 27 | −28.45 | 0.15 | 49.1 |
| 7.300 | 7.310 | S17-M6-B | humic | GrM-23831 | 0.4527 | 0.0016 | 6365 | 30 | −28.23 | 0.15 | 50.3 |
| 7.290 | 7.300 | S17-M5-B | humic | GrM-23832 | 0.4486 | 0.0016 | 6439 | 29 | −28.45 | 0.15 | 56.8 |
| 7.280 | 7.290 | S17-M4-B | humic | GrM-24024 | 0.4585 | 0.0016 | 6264 | 29 | −27.49 | 0.15 | 9.3 |
| 7.210 | 7.220 | S17-M12-B | humic | GrM-24025 | 0.4408 | 0.0016 | 6580 | 29 | −26.79 | 0.15 | 15.7 |
| 7.200 | 7.210 | S17-M11-B | humic | GrM-23865 | 0.4346 | 0.0016 | 6695 | 30 | −26.99 | 0.15 | 20.9 |
| 7.190 | 7.200 | S17-M3-B | humic | GrM-23866 | 0.4465 | 0.0016 | 6477 | 30 | −27.30 | 0.15 | 15.0 |
| 7.170 | 7.180 | S17-M1-B | humic | GrM-23867 | 0.4383 | 0.0016 | 6625 | 30 | −27.57 | 0.15 | 22.1 |
| 7.495 | 7.505 | S17-M9 | CPR | GrM-23521 | 0.5791 | 0.0017 | 4388 | 24 | −26.32 | 0.15 | 66.1 |
| 7.485 | 7.495 | S17-M8 | CPR | GrM-23522 | 0.5786 | 0.0019 | 4395 | 26 | −26.55 | 0.15 | 61.5 |
| 7.475 | 7.485 | S17-M7 | CPR | GrM-23523 | 0.5315 | 0.0018 | 5077 | 27 | −27.85 | 0.15 | 67.1 |
| 7.300 | 7.310 | S17-M6 | CPR | GrM-23491 | 0.4032 | 0.0041 | 7300 | 80 | NA | NA | NA |
| 7.280 | 7.290 | S17-M4 | CPR | GrM-23524 | 0.4097 | 0.0016 | 7168 | 30 | −26.30 | 0.15 | 64.0 |
| 7.210 | 7.220 | S17-M12 | CPR | GrM-23492 | 0.3513 | 0.0033 | 8400 | 80 | NA | NA | NA |
| 7.200 | 7.210 | S17-M11 | CPR | GrM-23525 | 0.3556 | 0.0013 | 8305 | 30 | −25.42 | 0.15 | 63.1 |
| 7.190 | 7.200 | S17-M3 | CPR | GrM-23493 | 0.3528 | 0.0036 | 8370 | 80 | NA | NA | NA |

**Table 8**
Dating results for core S18. CPR = charred plant remains, NA = not available.

| From (m O.D.) | To (m O.D.) | Sample name | Dated fraction | Lab-ID | $F^{14}C$ | ± (1σ) | $^{14}C$ age (yrBP) | ± (1σ) | $\delta^{13}C$ (IRMS) | ± (1σ) | %C |
|---|---|---|---|---|---|---|---|---|---|---|---|
| 11.80 | 11.81 | S18-M12-B | humin | GrM-23819 | 0.8017 | 0.0022 | 1775 | 22 | −27.79 | 0.15 | 49.9 |
| 11.79 | 11.80 | S18-M11-B | humin | GrM-23820 | 0.7969 | 0.0021 | 1823 | 22 | −28.20 | 0.15 | 24.4 |
| 11.78 | 11.79 | S18-M10-B | humin | GrM-23822 | 0.7979 | 0.0022 | 1814 | 22 | −28.13 | 0.15 | 42.9 |
| 11.77 | 11.78 | S18-M9-B | humin | GrM-23825 | 0.7971 | 0.0028 | 1821 | 29 | −27.74 | 0.15 | 38.0 |
| 11.73 | 11.74 | S18-M8-B | humin | GrM-23826 | 0.6973 | 0.0022 | 2896 | 26 | −27.30 | 0.15 | 20.1 |
| 11.72 | 11.73 | S18-M7-B | humin | GrM-24009 | 0.8177 | 0.0044 | 1615 | 45 | NA | NA | 1.4 |
| 11.71 | 11.72 | S18-M6-B | humin | GrM-24010 | 0.9203 | 0.0049 | 665 | 45 | NA | NA | 2.8 |
| 11.70 | 11.71 | S18-M5-B | humin | GrM-24011 | 0.5993 | 0.0035 | 4115 | 45 | NA | NA | 2.8 |
| 11.68 | 11.69 | S18-M4-B | humin | GrM-24012 | 0.6145 | 0.0033 | 3910 | 45 | NA | NA | 0.08 |
| 11.67 | 11.68 | S18-M3-B | humin | GrM-24013 | 0.5070 | 0.0028 | 5455 | 45 | NA | NA | 2.4 |
| 11.66 | 11.67 | S18-M2-B | humin | GrM-24014 | 0.6602 | 0.0036 | 3335 | 45 | NA | NA | 0.05 |
| 11.65 | 11.66 | S18-M1-B | humin | GrM-24015 | 0.8293 | 0.0048 | 1505 | 45 | NA | NA | 0.05 |
| 11.80 | 11.81 | S18-M12-B | humic | GrM-23499 | 0.7958 | 0.0064 | 1840 | 60 | NA | NA | NA |
| 11.79 | 11.80 | S18-M11-B | humic | GrM-23868 | 0.7963 | 0.0021 | 1830 | 21 | −27.91 | 0.15 | 49.0 |
| 11.78 | 11.79 | S18-M10-B | humic | GrM-23870 | 0.7938 | 0.0020 | 1855 | 21 | −28.22 | 0.15 | 53.4 |
| 11.77 | 11.78 | S18-M9-B | humic | GrM-23871 | 0.7790 | 0.0021 | 2006 | 22 | −28.66 | 0.15 | 53.2 |
| 11.73 | 11.74 | S18-M8-B | humic | GrM-23872 | 0.7117 | 0.0019 | 2732 | 22 | −28.35 | 0.15 | 49.1 |
| 11.72 | 11.73 | S18-M7-B | humic | GrM-23873 | 0.6861 | 0.0021 | 3026 | 24 | −28.31 | 0.15 | 38.2 |
| 11.71 | 11.72 | S18-M6-B | humic | GrM-23875 | 0.6029 | 0.0019 | 4064 | 26 | −28.04 | 0.15 | 36.6 |
| 11.70 | 11.71 | S18-M5-B | humic | GrM-23878 | 0.5718 | 0.0019 | 4491 | 26 | −28.31 | 0.15 | 36.3 |
| 11.68 | 11.69 | S18-M4-B | humic | GrM-23879 | 0.5526 | 0.0018 | 4765 | 26 | −28.93 | 0.15 | 39.8 |
| 11.67 | 11.68 | S18-M3-B | humic | GrM-23880 | 0.5410 | 0.0018 | 4935 | 27 | −28.91 | 0.15 | 37.9 |
| 11.66 | 11.67 | S18-M2-B | humic | GrM-23881 | 0.5380 | 0.0018 | 4980 | 27 | −29.06 | 0.15 | 32.0 |
| 11.65 | 11.66 | S18-M1-B | humic | GrM-23882 | 0.5512 | 0.0018 | 4785 | 26 | −29.16 | 0.15 | 28.5 |
| 11.79 | 11.80 | S18-M11 | CPR | GrM-23287 | 0.7902 | 0.0024 | 1892 | 24 | −28.18 | 0.15 | 62.9 |
| 11.73 | 11.74 | S18-M8 | CPR | GrM-23827 | 0.6863 | 0.0020 | 3024 | 24 | −27.69 | 0.15 | 64.0 |
| 11.72 | 11.73 | S18-M7 | CPR | GrM-23828 | 0.6659 | 0.0020 | 3267 | 24 | −27.62 | 0.15 | 62.2 |

process, basal peat layer and end of the peat initiation process (i.e., as based on %OM data, see Fig. 7) were specified in the P_Sequence. If no macrofossil date for these levels was available, the Date command was added as query to generate an age distribution. The Difference command was used to calculate a distribution for the amount of time that passed between the start and end of the peat initiation process. A t-type outlier model (Bronk Ramsey, 2009) using a T(5) distribution and U(0,4) scale was combined with the P_Sequence. The t-type outlier model is intended for cases where the measured sample might not relate to the event being dated (Bronk Ramsey, 2009). The prior probability for a macrofossil date to be an outlier was set to 5% (i.e., one out of twenty might be an outlier). The resulting age-depth models were calculated based on a model averaging approach, where macrofossil dates that are more probable to be outliers are down-weighted (Bronk Ramsey, 2009). See the Data Availability Statement for the OxCal scripts.

The likelihoods of humic and humin ages were plotted together with the macrofossil-based P_Sequences. The degree of overlap of the humic/humin likelihoods with the 95.4% confidence interval of the

**Table 9**
Dating results for core S20. CPR = charred plant remains, NA = not available.

| From (m O.D.) | To (m O.D.) | Sample name | Dated fraction | Lab-ID | F14C | ± (1σ) | $^{14}$C age (BP) | ± (1σ) | $\delta^{13}$C (IRMS) | ± (1σ) | %C |
|---|---|---|---|---|---|---|---|---|---|---|---|
| 10.38 | 10.39 | S20-M10-B | humin | GrM-23798 | 0.7686 | 0.0043 | 2115 | 45 | −28.06 | 0.15 | 49.1 |
| 10.37 | 10.38 | S20-M9-B | humin | GrM-23799 | 0.7692 | 0.0023 | 2108 | 24 | −28.55 | 0.15 | 47.2 |
| 10.36 | 10.37 | S20-M8-B | humin | GrM-23800 | 0.7693 | 0.0023 | 2107 | 24 | −27.04 | 0.15 | 27.8 |
| 10.35 | 10.36 | S20-M7-B | humin | GrM-23801 | 0.7423 | 0.0022 | 2394 | 24 | −28.10 | 0.15 | 37.5 |
| 10.33 | 10.34 | S20-M12-B | humin | GrM-23802 | 0.7131 | 0.0024 | 2716 | 27 | −29.16 | 0.15 | 16.2 |
| 10.32 | 10.33 | S20-M11-B | humin | GrM-23803 | 0.6628 | 0.0020 | 3304 | 24 | −28.60 | 0.15 | 26.7 |
| 10.31 | 10.32 | S20-M6-B | humin | GrM-23812 | 0.6608 | 0.0020 | 3328 | 24 | −29.69 | 0.15 | 29.5 |
| 10.30 | 10.31 | S20-M5-B | humin | GrM-23813 | 0.6518 | 0.0021 | 3438 | 26 | −30.09 | 0.15 | 34.9 |
| 10.29 | 10.30 | S20-M4-B | humin | GrM-24006 | 0.7512 | 0.0022 | 2298 | 24 | NA | NA | 7.7 |
| 10.26 | 10.27 | S20-M3-B | humin | GrM-24007 | 0.7451 | 0.0043 | 2365 | 45 | NA | NA | 2.4 |
| 10.25 | 10.26 | S20-M2-B | humin | GrM-23737 | 0.6413 | 0.0033 | 3570 | 40 | NA | NA | 13.2 |
| 10.24 | 10.25 | S20-M1-B | humin | GrM-24008 | 0.7963 | 0.0040 | 1830 | 40 | NA | NA | 1.3 |
| 10.38 | 10.39 | S20-M10-B | humic | GrM-23968 | 0.7723 | 0.0021 | 2076 | 22 | −28.07 | 0.15 | 53.4 |
| 10.37 | 10.38 | S20-M9-B | humic | GrM-24018 | 0.7707 | 0.0025 | 2093 | 26 | −27.94 | 0.15 | 42.8 |
| 10.36 | 10.37 | S20-M8-B | humic | GrM-24017 | 0.7543 | 0.0026 | 2265 | 27 | −26.83 | 0.15 | 16.6 |
| 10.33 | 10.34 | S20-M12-B | humic | GrM-23883 | 0.6954 | 0.0021 | 2918 | 24 | −28.05 | 0.15 | 35.1 |
| 10.32 | 10.33 | S20-M11-B | humic | GrM-24019 | 0.6635 | 0.0025 | 3295 | 30 | −28.20 | 0.15 | 27.8 |
| 10.31 | 10.32 | S20-M6-B | humic | GrM-23884 | 0.6530 | 0.0021 | 3424 | 26 | −28.22 | 0.15 | 49.1 |
| 10.30 | 10.31 | S20-M5-B | humic | GrM-24021 | 0.6419 | 0.0022 | 3561 | 27 | −28.77 | 0.15 | 46.7 |
| 10.29 | 10.30 | S20-M4-B | humic | GrM-23969 | 0.6473 | 0.0033 | 3495 | 40 | −29.29 | 0.15 | 32.7 |
| 10.26 | 10.27 | S20-M3-B | humic | GrM-23885 | 0.6247 | 0.0020 | 3779 | 26 | −29.11 | 0.15 | 30.0 |
| 10.25 | 10.26 | S20-M2-B | humic | GrM-24022 | 0.6135 | 0.0020 | 3924 | 27 | −28.75 | 0.15 | 14.9 |
| 10.24 | 10.25 | S20-M1-B | humic | GrM-23886 | 0.6290 | 0.0023 | 3725 | 29 | −28.85 | 0.15 | 20.2 |
| 10.37 | 10.38 | S20-M9 | CPR | GrM-23814 | 0.7580 | 0.0020 | 2225 | 22 | −24.54 | 0.15 | 66.4 |
| 10.36 | 10.37 | S20-M8 | CPR | GrM-23815 | 0.7577 | 0.0020 | 2229 | 22 | −25.24 | 0.15 | 63.9 |
| 10.33 | 10.34 | S20-M12 | CPR | GrM-23208 | 0.6962 | 0.0027 | 2910 | 30 | −26.94 | 0.15 | 60.6 |
| 10.32 | 10.33 | S20-M11 | CPR | GrM-23817 | 0.6746 | 0.0022 | 3163 | 26 | −26.90 | 0.15 | 71.3 |
| 10.31 | 10.32 | S20-M6 | CPR | GrM-23818 | 0.6906 | 0.0021 | 2974 | 24 | −26.53 | 0.15 | 63.1 |

P_Sequences indicates the accuracy of the humic/humin dates in representing the age of the peat layer from which they were obtained.

## 3. Results

### 3.1. The organic matter gradient of the mineral-to-peat transition: defining basal peat ($M_d$)

The five vertical series of LOI measurements to derive the OM gradient at the mineral-to-peat transition are shown in Fig. 6. The data show a clear and abrupt rise of OM over a distance of a few cm. Based on this outcome *peat* was defined as material with an OM percentage of 40% or higher (i.e., the defining value $M_d = 40\%$). The layer called *basal peat* is therefore the first cm of material with OM $\geq$ 40%.

### 3.2. Plant macrofossils (PM) and testate amoebae (TA)

Overall the samples that originated from the stratigraphical layer described as amorphous organic matter (Table 2) contained few macrofossils. In the non-decomposed (waterlogged) peat (Table 2) mostly belowground remains such as rootlets, radicelle and rhizomes were preserved. Few waterlogged aboveground plant tissues were present, however charred aboveground remains could often be identified (Table 6).

In general, all investigated levels of the three cores contained small unidentifiable rootlets. Part of the rootlets was of Cyperaceous origin, of which some were identified as *Carex* radicelle. The bottom levels of S18 and S20 contained fine sand, and in some of these levels also sclerotia of the mycorrhizal fungus *Cenococcum geophilum* were present. In the core of lowest elevation, S17, the bottom levels (7.17–7.20 m O.D.) contained a few leaves of *Sphagnum austinii* (*S. imbricatum*) and six megaspores of *Selaginella selaginoides*. From 7.20 to 7.22 m O.D. many charred herbaceous stems were present, of which some likely derived from stem bases (corm) of *Eriophorum*. Slightly higher in the profile (7.28–7.31 m O.D.) fewer herbaceous stems were observed and many sclerotia of the fungus *Cenococcum geophilum* were found. The upper three levels, from 7.475 to 7.505 m O.D., contained vegetative remains of *Eriophorum vaginatum*, *Erica tetralix*, *Calluna vulgaris*, *Bryales* species, *Sphagnum austinii* and other *Sphagnum* species. In core S20, between 10.30 and 10.34 m O.D., leaf and/or stem remains of Poaceae (including *Phragmites* and other species) were present, which were not found in core S17 and S18. In the upper levels of cores S18 and S20, charred herbaceous stems and twigs of *Calluna vulgaris* and/or *Erica tetralix* were found. In addition, the upper levels of core S20 contained some stems of *Bryales* mosses, whereas in core S18 some charred *Sphagnum* stems were found. Both core S18 and S20 contained waterlogged seeds of *Juncus* (*Juncus conglomeratus/effusus*) in their upper levels.

Almost none of the investigated levels contained suitable material for testate amoebae analyses. In four subsamples only a few damaged or broken tests were present, which could be identified as *Difflugia pristis* or other *Difflugia* species.

### 3.3. Dating results

The radiocarbon dating results for the investigated levels for each core are shown in Tables 7–9. The calibrated ages, modelled P_Sequences, and OM content are shown in Fig. 7. Overall, the chronological order of the dates from macrofossils concurs with stratigraphical position (older at the bottom and younger towards the top). However, there is one reversal in core S20 at 10.31–10.32 m O.D.. The chronological order of the humic dates is also largely correct, with a few exceptions of minor reversals (S17: 7.19 and 7.28 m O.D.; S18: 11.65 m. O.D.; S20: 10.24 m. O.D.). For higher levels (above the mineral-to-peat transition), humin ages converge with those based on humics and plant macrofossils. For lower levels however, humin ages are scattered.

Dates of plant macrofossils, humics and humins diverge for samples from the mineral-to-peat transition (i.e., in Fig. 7 between 'Start of peat initiation process' and 'End of peat initiation process'), especially for core S17. The higher in the profile and the further away from the mineral-to-peat transition, dates of plant macrofossils and both humic and humin fractions are increasingly in agreement. At the levels where the radiocarbon ages diverge, dates of plant macrofossils represent the oldest fraction in cores S17 and S18. For core S17 the difference between the macrofossils and humics is relatively constant for the samples below

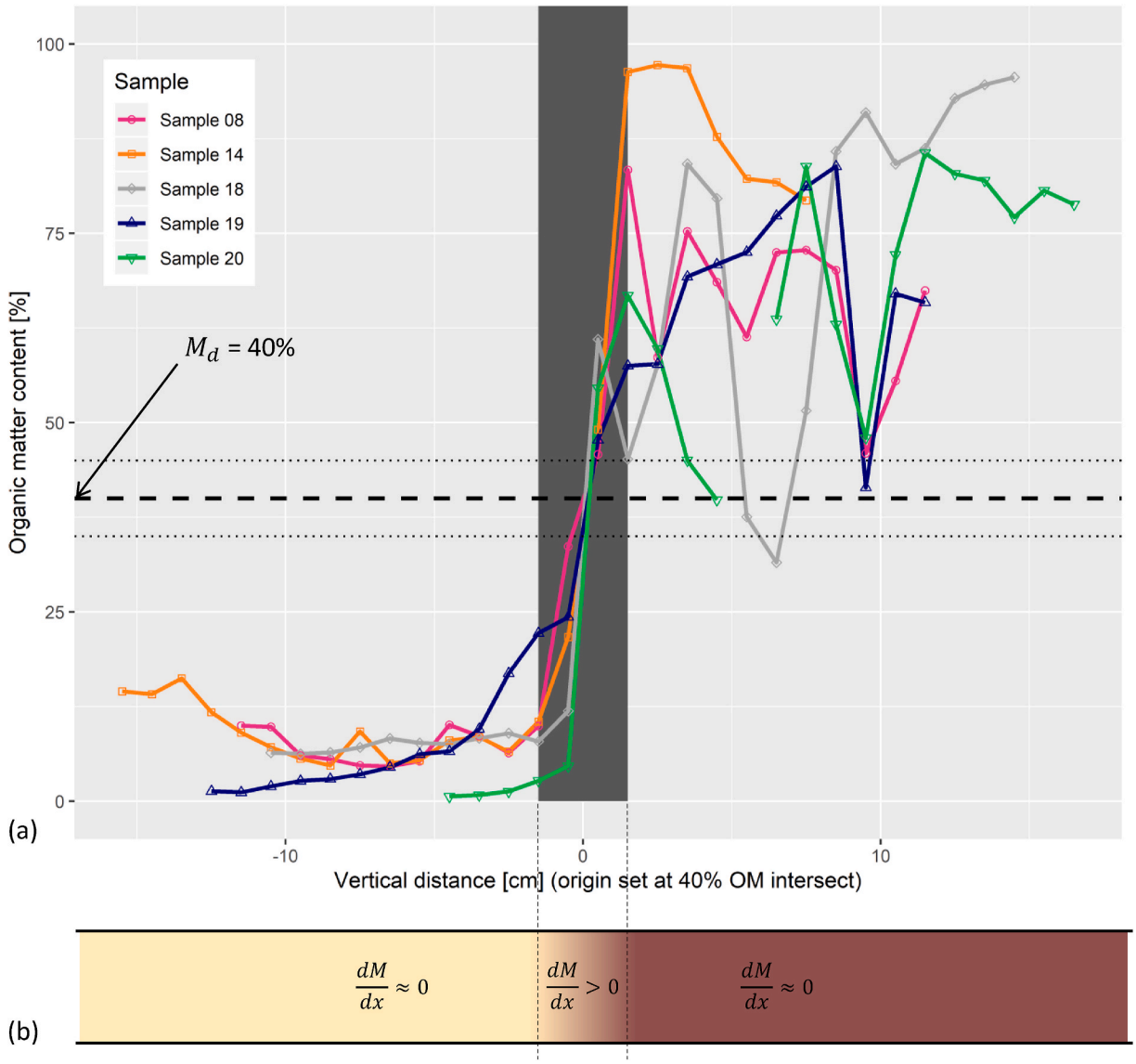


**Fig. 6.** (a) Organic matter data of five cores (for locations, see Fig. 2). The dashed horizontal line shows the value of $M_d$, which was set at 40% OM. The dotted horizontal lines indicate an OM content of 35% and 45% for ease of comparison. For one 1-cm-thick layer of core 20 no data were available, this causes the discontinuity in the green line. (b) Schematic core rotated 90° clockwise, showing conceptual organic matter gradient (see also Fig. 1b).

7.22 m O.D., while also the dates of these fractions are relatively constant with increasing depth. In core S20, no plant macrofossils were available from the sandy layers at the bottom. Here, the humics are generally oldest, humin ages are very dispersed.

The part of the stratigraphy with the rising OM gradient ('period of peat initiation' as explained in Fig. 1b, also see Fig. 6) reflects the timespan (duration) of the peat initiation process. Based on the P_Sequences presented in Fig. 7, this timespan was modelled (Fig. 8). Results show that the peat initiation process took a median of 1073 years at the location of core S17 (91–2706 years at 95.4% probability). At the site of S20 the process took a bit longer with a median duration of 1343 years (472–2040 at 95.4%). The process took longest at site S18, here the median lies at 1510 years (1301–1714 years at 95.4%).

## 4. Discussion

Here we discuss the process of peat initiation as reflected by the mineral-to-peat transition in the stratigraphical record, the resulting definition of *basal peat* (4.1), followed by the reconstructed palaeoenvironment (4.2), the course and timespan of peat initiation (4.3), and the age assemblage of the different carbon fractions (4.4). Based on this, recommendations for dating *basal peat* are formulated (4.5).

### 4.1. Mineral-to-peat transition and basal peat (defining $M_d$)

Our analyses demonstrate that the organic matter content shows a clear and steep rise over a distance of a few centimetres, starting at low values of about 10% and increasing to more than 90% (Fig. 6). This gradient reflects the stratigraphical mineral-to-peat transition. The drastic rise in OM content occurs around an OM percentage of 40%. In the explanation of the Dutch soil classification system by De Bakker and Schelling (1966), a range of organic matter classes is defined based on OM and clay percentages (by mass). For soils containing 0–8% clay (as in our case study area), the material is called *peat* when containing >35% OM (in case of 8% clay) or >40% OM (when containing 0% clay). This is in strong agreement with the results of our LOI tests (Fig. 6), based on which we have selected 40% OM as cut-off value ($M_d$) above which we define the material as *peat*. The first 1-cm-thick subsample that contained ≥40% OM is therefore defined as the *basal peat* layer.

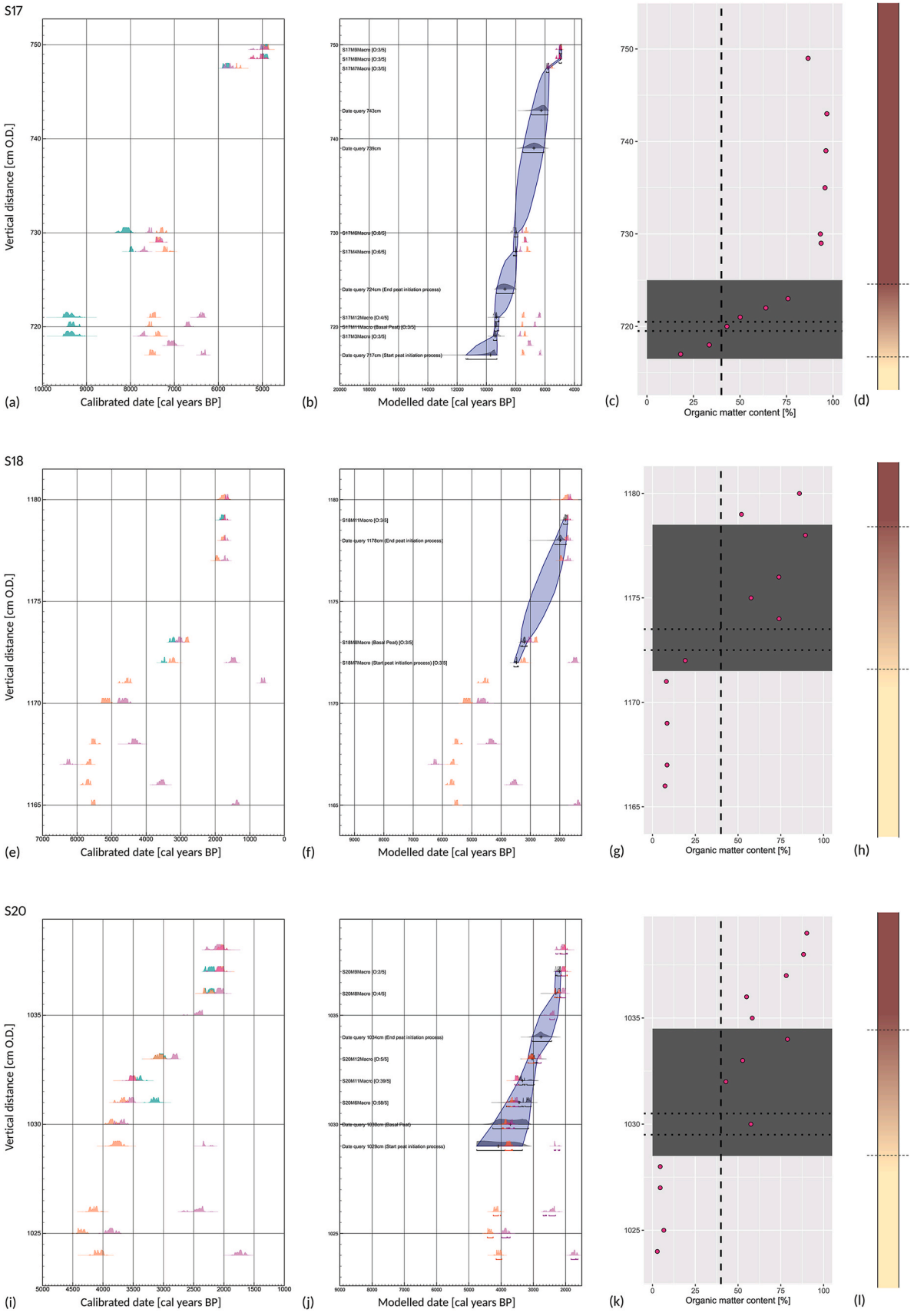


*(caption on next page)*

**Fig. 7.** Overview of dating results and OM percentages for core S17 (a–d), S18 (e–h) and S20 (i–l). (a/e/i) Age-depth plot showing the likelihoods of all dated fractions; green = macrofossils, orange = humics, pink = humins. Note that some likelihoods overlap, see Tables 7–9 for an overview of all dated fractions per layer. (b/f/j) Age-depth plot showing the result of a P_Sequence based on macrofossil dates, accompanied with an outlier model (see Methods for details). The probability for a date to be an outlier is indicated behind each date at the left side of the plot in the format [O:x/5], where x gives the posterior probability and 5 the prior probability that was entered in the outlier model (always set to 5%). Blue shading = 95.4% confidence interval, + = median of modelled posterior distribution, orange = likelihood of humics, pink = likelihood of humins. Degree of overlap of the humic/humin likelihoods with the confidence interval of the P_Sequence indicates accuracy of the humic/humin dates in representing the age of the peat layer from which they were obtained. (c/g/k) Organic matter data, the combination of dashed and dotted lines indicates which sample is the first with OM ≥ 40%, dark grey shading = samples that encompass the peat initiation process (mineral-to-peat transition). (d/h/l) Schematic cores showing conceptual stratigraphy as in Fig. 1b and 6b.

### 4.2. Palaeoenvironment

The investigated cores contained a limited amount of well-preserved plant macrofossils. Part of these remains is charred (Table 6). In several levels sclerotia of *Cenococcum geophilum*, a mycorrhizal fungus that usually lives in the sandy subsoil, were observed (Table 6). In peat, the presence of *C. geophilum* may indicate relatively dry conditions (Van Geel, 1978). Presence of charred and uncharred plant remains in multiple levels of the cores suggests (local) wildfires (for more information on (palaeo)wildfires in peatlands see e.g. Zaccone et al., 2014; Nelson et al., 2021; Rein and Huang, 2021). Dry periods allow further breakdown of material, which could explain the rather poor preservation of uncharred (waterlogged) macrofossils.

It is important to note that even though a bog remnant is studied here, the *basal peat* is in fact fen peat (which is quite often the case; see e.g. Korhola, 1994; Cubizolle et al., 2007). The mineral-to-peat transition is later followed by a fen-bog transition as a result of ombrotrophication (for more information on the latter transition see e.g. Almquist-Jacobson and Foster, 1995; Hughes, 2000; Hughes and Barber, 2004; Väliranta et al., 2017; Loisel and Bunsen, 2020). Our findings indicate that at all three cored locations the peat-forming vegetation was initially mesotrophic. The local vegetation was dominated by sedges, with some presence of *Juncus* (Table 6). After the peat initiation process, conditions became more oligotrophic, and the vegetation at S17 and S18 developed probably to an oligotrophic bog with *Calluna vulgaris*, *Erica tetralix* and *Sphagnum* (ombrotrophic conditions). At the location of S20 no *Sphagnum* remains were found, but the vegetation likely changed to a moss (*Bryales*) and heather vegetation.

The investigated cores appeared to be very low in testate amoebae content. However, the presence of *Difflugia* species in a few samples suggests very wet conditions. This taxon and the presence of abundant diatoms (which were observed during TA analysis but not subject of further study) suggest a fen environment (rather than an ombrotrophic bog), which is in agreement with the botanical data. Testate amoebae are often poorly preserved under fen-type conditions, possibly due to predation, physical disaggregation or chemical dissolution, or a combination of these (Roe et al., 2002; Swindles and Roe, 2007; Swindles et al., 2020).

In the investigated levels, *C. geophilum* does not occur simultaneously with *Difflugia* species. This mutual exclusion suggests respectively drier and wetter conditions that alternated during the timespan of the peat initiation process. Additionally, a detailed study by Sullivan and Booth (2011) has shown that several *Difflugia* species (including *D. pristis*) are able to cope with fairly high levels of short-term variability in environmental conditions at the peat surface. This variability appeared to be higher at locations with loose-growing *Sphagnum* (rather than dense *Sphagnum* cover) or where vegetation was dominated by vascular plants and non-*Sphagnum* bryophytes (Sullivan and Booth, 2011). We suggest that such conditions may be similar to those in our study area during peat initiation and the transition to an oligotrophic bog.

### 4.3. Timespan of the peat initiation process

The stratigraphical reach with the rising OM gradient (Figs. 1b and 6) reflects the timespan of the peat initiation process. Based on the P_Sequences in Fig. 7, these timespans were modelled for each core (Fig. 8). Results show that this process lasted for 1073, 1510 and 1343 years (medians) for core S17, S18, and S20 respectively. In the stratigraphy, this is reflected in a vertical distance of respectively 8, 7 and 6 cm. This means that apparent vertical accumulation during these first stages of peat development varied between the sites with values of 0.07, 0.05 and 0.04 mm/year for core S17, S18, and S20 respectively. A typical value given for the apparent peat accumulation rate in the catotelm is 1 mm/year, and may be lower further down in the catotelm due to compaction and anaerobic decomposition (Rydin and Jeglum, 2013c). A low apparent accumulation rate is indeed the case here, with rates far below 1 mm/year. This implies that 1 cm of peat, at the slowest rate of 0.04 mm/year, reflects about 250 years of peat growth.

Very few studies have investigated the timespan that is reflected in the first centimetres above the layer they define as *basal peat*. For two cores, Berendsen et al. (2007) dated a pair of vertically spaced samples (taken 11 cm apart in one core and 9 cm apart in the other), and found age differences of respectively 60 and 120 calendar years. Based on this, they conclude that within-core sampling resolution is less critical than previously assumed.

The difference between our results and those of Berendsen et al. (2007) highlights that the peat initiation process cannot be assumed to be rapid in all cases and is influenced by environmental setting. Depending on the timespan of the peat initiation process and the apparent accumulation rate, a high vertical sampling resolution and small sample thickness can be crucial to obtain accurate dates. The duration of peat initiation also determines to which degree a date of *basal peat* is representative to use as starting point for build-up of peat deposits.

It is important to note that the reconstructed timespans and apparent accumulation rates are based on age-depth relationships (instead of a mass-age relationship). These age-depth relationships do not consider gross accumulation and subsequent decay separately, but only the apparent vertical increase (potentially affected by decomposition and/or compaction). Due to water-saturated conditions for significant periods of time, bioturbation by soil fauna is presumably low during the peat initiation process. This assumption is corroborated by the intact chronostratigraphy of macrofossils shown in our cores (Fig. 7a/e/i). As the timespan of the peat initiation process is potentially long, we emphasize that sampling resolution and sample thickness are key points to consider when dating the start of peat growth.

### 4.4. Age assemblage of carbon fractions

Our data demonstrate that macrofossils (i.e., *in situ* material) in the *basal peat* layer are oldest, and that both humics and humins generally show younger ages. In line with the general consensus in literature (e.g. Piotrowska et al., 2011), we consider the macrofossils to reflect the 'true' age, i.e. representative for the timing when the vegetation accumulated at the specific location. Aboveground remains (no roots) of terrestrial plants are expected to have been in equilibrium with atmospheric $^{14}C$ values until they died and we therefore do not expect any reservoir effect (also see Blaauw et al., 2004). In this study, samples were carefully selected, cleaned and pre-treated with the full ABA-protocol to minimise the presence of any contamination with carbon from sources other than the original plant materials (see sections 2.5 and 2.8). The macrofossils show a clear chronological order, with samples dating

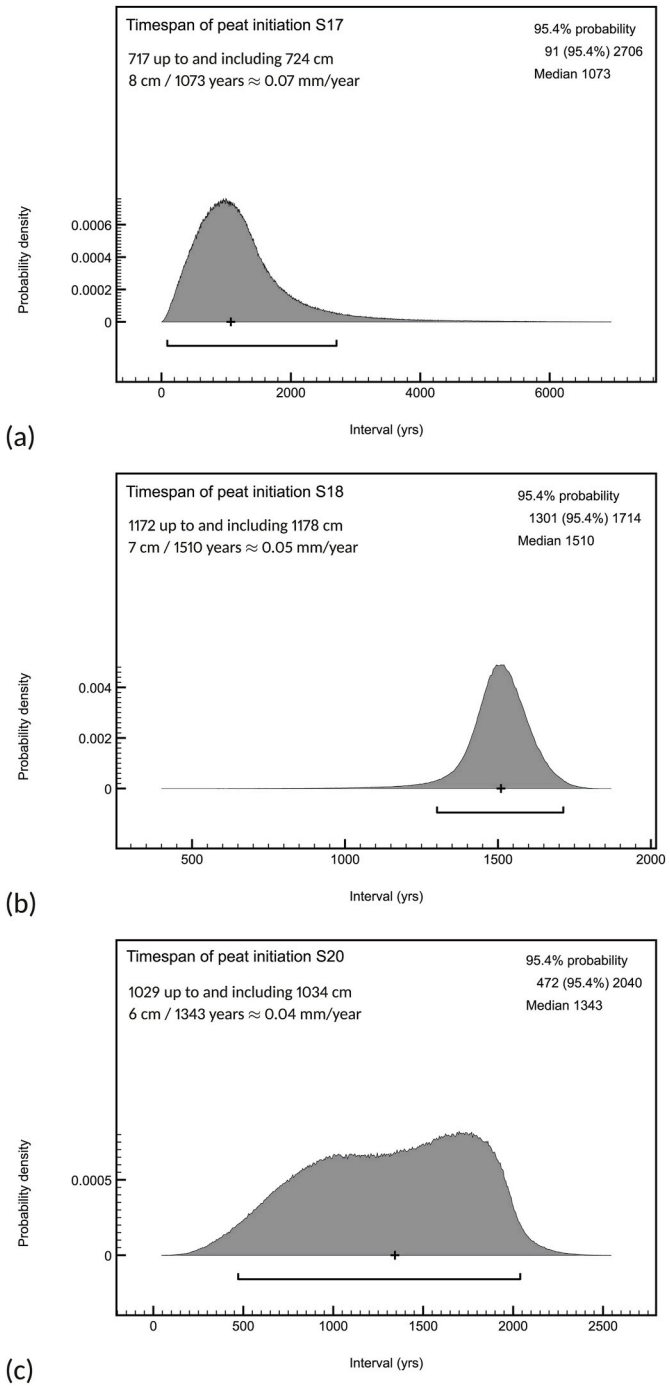


**Fig. 8.** Timespan (duration in years) of the peat initiation process in cores S17, S18 and S20, derived from the P_Sequence models shown in Fig. 7(b/f/j) (see Methods for details). Apparent accumulation rate (expressed in mm/year) was calculated by dividing the stratigraphical distance of the peat initiation process (provided in cm, see also Fig. 7(b/f/j)) by the modelled median of the timespan. Note that these accumulation rates are based on an age-depth relationship (instead of a mass-age relationship) and do not consider gross accumulation and subsequent decay separately, but only the apparent vertical increase (potentially affected by decomposition and/or compaction).

younger upwards in the profile, which suggests that macrofossil relocation through bioturbation is unlikely. There is only one reversal for the macrofossils in core S20 at 10.31 m O.D., while the humic and humin fractions of this same layer do not show a deviation in chronology. The cause for this deviation remains unclear. The outlier model shows that there is an increased chance that either S20M11macro or S20M6macro is an outlier; through the model averaging approach these dates are corrected in the P_Sequence (Fig. 7j).

Despite the correct chronological order of the humic dates, the age difference between humics and plant macrofossils in core S17 from 7.19 to 7.30 m O.D. shows that the absolute humic ages are likely too young (Fig. 7a and b). This difference in age ranges from about 1700 to 800 years. The same applies to core S18 at depths 11.72 and 11.73 m O.D. (Fig. 7e and f), with age differences of about 250–400 years. This is different in core S20, where two humic samples dated older than macrofossils from the same layer. At 10.31 m O.D., the macrofossil sample deviates from the chronology (see above), which causes a fairly large difference with the humic age of approximately 530 years (Fig. 7i and j). At 10.32 m O.D. however, where the macrofossil date concurs with chronological order, the humic date is only about 120 years older.

The humins, both in the *basal peat* but also below in the Pleistocene deposits, show younger ages than the humics and plant macrofossils, and remarkably little coherence. In the sandy Pleistocene layers the organic matter content was low and sand content high. Separating this small amount of carbon from the sand in the lab appeared to be challenging, resulting in several humin samples with fairly low %C (Tables 7–9). If some younger material is incorporated here, the influence on the resulting age will be larger due this small sample size. This may account for part of the observed variation.

Overall, both the humic and humin fractions derived from the mineral-to-peat transition result in younger ages. Fluctuating water tables during the process of peat initiation (discussed above), might explain the origin of younger carbon in these first peat layers. Changes in hydraulic head may lead to both upward and downward (and also sideward) movement of soluble organic compounds (Waddington and Roulet, 1997). Low water levels specifically allow downward water movement through the profile, potentially transporting mobile humic acids that contain young carbon to lower levels. As the mobility of humics is pH-dependent (Wüst et al., 2008), the initial mesotrophic conditions allow higher mobility than the more acid, ombrotrophic conditions that follow later in time (see above).

Brock et al. (2011) dated humic and humin fractions from three grain sizes obtained through wet-sieving (63–125 μm, 125–250 μm and >250 μm), originating from a 1-cm-thick layer positioned 1 cm below the level they regarded to reflect peat initiation. Their results show that for two of these grain sizes, the humic and humin dates are not significantly different from each other. However, both the dates of the humics and the humins become older with increasing grain size, suggesting that the fine particulate matter may be responsible for younger contaminations in both fractions. In our study, the bulk material was not sieved during the entire pre-treatment procedure, to secure that the very small organic particles in the bulk material were retained. Presence of this fine fraction may be responsible for the observed younger dates of the humics and humins, but does not explain the erratic pattern of the humin dates.

Downgrowth of roots may also cause age differences in bulk samples compared to aboveground plant macrofossils, a problem that appears to be of particular relevance in the case of slowly accumulating (fen) peat (Streif, 1972; Törnqvist et al., 1992) such as encountered here during the peat initiation process. The effect may also depend on the botanical composition of the peat-forming vegetation, as certain species such as *Phragmites* or *Eriophorum vaginatum* (Table 6) can produce fairly deep roots (Kohzu et al., 2003; Iversen et al., 2015). As humics and humins result from decomposition, their ages may result partly from *in situ* carbon and partly from younger carbon that originated from mobile fulvic and humic acids and roots. Additional dating of separated rootlets at multiple levels slightly above the mineral-to-peat transition may shed more light on the sources of error in the ages of the humics and humins for dating peat initiation.

Holmquist et al. (2016), who compared radiocarbon dating results for plant macrofossil and bulk samples obtained from basal peat in circum-arctic peatlands, found no significant difference in ages. Based on this they conclude that evidence for a consistent systematic bias

introduced by the incorporation of bulk peat dates in large basal $^{14}C$ databases from peatlands is lacking. In contrast, the large age difference between dates of plant macrofossils and humic or humin dates (up to ~1700 years between macrofossil and humic ages in our case study peatland, and with even larger differences for humins, Fig. 7a and e) indicates that studies reusing existing bulk dates of *basal peat* should take great care in data interpretation. Some of these studies, which concentrate on regional or global reconstructions of peat initiation (e.g. Tolonen and Turunen, 1996; Macdonald et al., 2006; Ruppel et al., 2013), have important implications for climate research and carbon budgets. Depending on the sample type obtained from the dated *basal peat* layers, dates are potentially interpreted more safely as terminus-ante-quem dates for peat initiation, or should be subjected to rigorous quality assessment prior to data analysis (Quik et al., 2021).

Higher in the peat profile however, dates of plant macrofossils, humics and humins converge, indicating homogeneity regarding carbon fractions and ages. Some of these dates do not differ significantly, others fall within a (very) short timeframe (Fig. 7b/f/j). We suggest that as water tables started fluctuating less, peat accumulation speed began to increase, and conditions became more ombrotrophic (start of *Sphagnum* growth, Table 6). As a result, downward water flow declined and mobility of humics decreased. In line with Törnqvist et al. (1992) and Blaauw et al. (2004), our findings suggest that when focus is not directed towards the *basal peat*, but to higher layers in the peat profile that are characterised by more stable water tables and higher accumulation rates, one might obtain accurate dates through bulk sampling (both humics and humins).

In the mineral soil horizons, i.e. those with <40% OM, generally no (aboveground) plant remains could be recognized. Samples from the stratigraphical layers peaty sand/sandy peat and Pleistocene deposits (i.e., the palaeosoil that became covered with peat, Table 2) could therefore only be radiocarbon dated using the humic and humin fractions. Humic acids are considered to be the most reliable fraction for dating organic matter in soils if no plant remains and (almost) no organic carbon is present (Van der Plicht et al., 2019). Indeed, the humin ages of the Pleistocene layers display poor coherence (Fig. 7) with frequent stratigraphical inconsistencies. Humic ages in contrast provide results that are stratigraphically consistent. In core S18 for example (Fig. 7e), the four humic samples between 11.65 and 11.69 m O.D. all date around 5500 cal y BP. This consistency could suggest that these samples represent the slow build-up of organic matter in the sandy soil (i.e., at the time prior to peat growth). Some of the humin dates in the mineral horizons show remarkably young ages, perhaps due to the small amount of total carbon in these samples as mentioned above (Tables 7–9), and relatively larger quantities of carbon from other carbon sources. Dating soil organic matter in mineral soils is complicated and involves different processes than peat initiation (see e.g. Goh and Molloy, 1978; Van Mourik et al., 1995; Van der Plicht et al., 2019), further study of these dates is therefore beyond the scope of the present study.

### 4.5. Recommendations for dating peat initiation

Our study highlights that peat initiation is a process rather than an event, which has implications for dating peat initiation and *basal peat*. This process is reflected in the stratigraphy as a gradual boundary between mineral sediments and overlying peat deposits. The mineral-to-peat transition can be characterised using the organic matter gradient ($\frac{dM}{dx}$, Fig. 1b). The use of biostratigraphical indicators to define *basal peat*, as for instance in the approach used by Törnqvist et al. (1998), is not always possible due to limited presence of plant macrofossils and potential lack of testate amoebae. However, if material is present and resources allow, including additional biostratigraphical analyses to characterise the palaeoenvironment of the peat initiation process is valuable.

The layer that is interpreted as *basal peat* should be defined clearly and quantitatively, which ensures reproducibility and eases intercomparison of studies. To move towards a quantitative definition of *basal peat*, a simple parameter such as OM is useful as it is easy to measure at low cost, which enables widespread use. Based on the obtained organic matter gradient ($\frac{dM}{dx}$) that reflects the peat initiation process, a value ($M_d$) can be chosen for the organic matter percentage above which the material is called *peat*. The first cm that has an OM% equal to or above this value is defined as the *basal peat* layer.

Based on our results, an $M_d$ value of 40% OM would be recommendable to define *basal peat* in areas comparable to our case study peatland. This value agrees very well with the Dutch soil classification (De Bakker and Schelling, 1966), especially given the low clay content of the soils in our study area (Table 2). However, for peatlands in other regions or with a different botanical composition near the base, LOI-testing may result in a different value for $M_d$.

As organic matter measurements using LOI require burning the subsample, care should be taken beforehand to ensure sufficient allocation of sample material to all required analyses. Additionally, it should be kept in mind that post-depositional changes such as downgrowth of roots may change OM content, therefore determining the OM gradient over a reach of several cm is useful to contextualise single measurements. We therefore highly recommend to investigate a stratigraphical range to properly contextualise the mineral-to-peat transition and for selecting an OM value to define the *basal peat*.

An additional advantage of organic matter content determination is that this information may help in estimating chances to obtain sufficient amounts of plant macrofossils for $^{14}C$ dating from specific layers. For the three cores investigated in this study, nearly all (12 out of 14) of the macrofossil samples for dating originated from layers with an organic matter content of 40% or higher. Most of the dated layers with OM below 40% did not contain sufficient macrofossils for dating and were dated solely using humics and humins. Depending on the organic matter gradient and local conditions, this potentially varies between study regions, but may be taken into account for sample selection.

Depending on the timespan of the peat initiation process and apparent accumulation rate, sampling resolution and sample thickness may affect the accuracy of dates in representing the start of peat growth. If accumulation rates are high, a lower vertical sampling resolution or sample size of several cm's might be adequate, whereas lower accumulation rates may require detailed sampling with small sample sizes depending on the research question to be answered. If the timespan of peat initiation and related apparent accumulation rate are unknown, studies aiming to date *basal peat* with a higher accuracy than several hundred (potentially thousand) years should take great care regarding vertical sampling resolution and sample size, as the assumption of a rapid process is not always valid.

An elaborate dating inventory comparable to the approach of the present study is valuable as it provides detailed information on the peat initiation process and on the accuracy of different carbon fractions for dating. To gain insight in the timespan of peat initiation, and consequently to ensure accurate dates of the peat initiation process and *basal peat*, dating several vertically spaced samples within one core as a preceding test is very useful. If time allows, such a layered or multi-stage approach for dating peat initiation and lateral expansion is recommendable (also see staged approaches for dating as suggested by Bayliss, 2009 and Piotrowska et al., 2011). For instance, after obtaining the OM gradient dating plant macrofossils and humics of three levels dispersed over the mineral-to-peat transition would allow substantiated choices for sampling size and resolution for subsequent spatial dating schemes. These preliminary dates and insights may be used to run simulations in OxCal to evaluate potential outcomes of alternate approaches for more extensive (spatial) sampling and dating. If a multi-stage approach is not possible and only one level of each core is dated without prior tests, assumptions on the timespan of peat initiation and related choices in

sampling resolution and sample size should be explicitly discussed.

Our findings show that plant macrofossils provide the most reliable age near the mineral-to-peat transition and the *basal peat* layer, and are therefore recommendable to use for $^{14}C$ dating. The full ABA pretreatment of macrofossils lowers the risk of chemical contamination and should be applied when possible. If plant macrofossils are unattainable, either due to poor preservation or limited resources for biostratigraphical analyses, dates of the humic fraction provide the best alternative regarding chronological order. These dates may however deviate from those of plant macrofossils, and our data show that humics can therefore only provide a terminus-ante-quem for the dated levels. If bulk samples are used, it is important to clearly report which fraction was obtained from the sample and used for dating. If marker layers such as tephra are present, these can be used to correlate sites or even provide independent age control if a date can be obtained for the event.

Above the mineral-to-peat transition, our results indicate that dating results of plant macrofossils, humics and humins converge. This implies that humics and humins might be a useful alternative to plant macrofossils for dating peat layers higher in the profile. Justifying this choice would however require a-priori dating knowledge of the peatland under study, and occasional cross-checks with macrofossil dates to ensure accuracy of results.

If the peatland under study is protected as a nature reserve (i.e., not a peat extraction site or location with an outcrop), digging a trench for sampling all the way down to reach the mineral-to-peat transition creates a large disturbance (and would be severely hampered by practical challenges with water infilling). Coring provides an efficient alternative, even though commonly used coring tools such as the Russian corer have a limited sample volume. This limits the options for dating in combination with multiproxy study at a high resolution (Piotrowska et al., 2011). This combination is possible (e.g. as in our study), but requires careful allocation of material to various analyses and involves dating (very) small samples. If chances for obtaining plant macrofossils are encouraging (e.g. based on OM%), one could choose to sacrifice the bulk subsample intended for dating and process it for plant macrofossil analysis. If the expectation regarding plant macrofossils is low, then keeping a bulk sample would offer the possibility to obtain at least a terminus-ante-quem for peat initiation using the humic fraction extracted from the bulk sample.

## 5. Conclusions

### 5.1. Dating peat initiation

In this study we aimed to formulate updated recommendations for dating peat initiation. We based our approach on a conceptual framework (Fig. 1) that supports the use of the organic matter (OM) gradient for a quantitative and reproducible definition of the mineral-to-peat transition (i.e., the stratigraphical range reflecting the timespan of the peat initiation process) and the layer defined as *basal peat* (i.e., the stratigraphical layer that is defined as the bottom of a peat deposit). Subsequently we analysed the mineral-to-peat transition for a case study peatland in the Netherlands, based on three detailed series of radiocarbon dates that include plant macrofossils, humics and humins. Our findings demonstrate that plant macrofossils, even though their presence in basal peat is often limited, provide the most reliable dating

**Textbox 1**
Summary of recommendations for dating peat initiation.

- Study the mineral-to-peat transition using the organic matter gradient, and if resources allow, by including biostratigraphical analyses (see [A] in the textbox figure below);
- Take the timespan of the peat initiation process into account when deciding upon sample size and sampling resolution. A layered or multistage approach is useful to gain insights on the duration of peat initiation prior to executing elaborate spatial dating schemes (see [B] and [C]);
- Define basal peat based on the organic matter gradient to obtain a low-cost, quantitative and reproducible definition that eases intercomparison of studies (see [D]);
- Regarding which fraction to use for 14C dating basal peat (see [E]), our data show that plant macrofossils provide the most accurate age in the mineral-to-peat transition and are therefore recommendable to use. If these are unattainable, dates of the humic fraction provide the best alternative regarding chronological order, but may deviate significantly from the 'true age'. Our results show that humic dates are best interpreted as terminus-ante-quem dates;
- Potentially limited options for sampling and resulting small sample volumes require detailed consideration of allocating material to analyses (see Fig. 5 for an example).

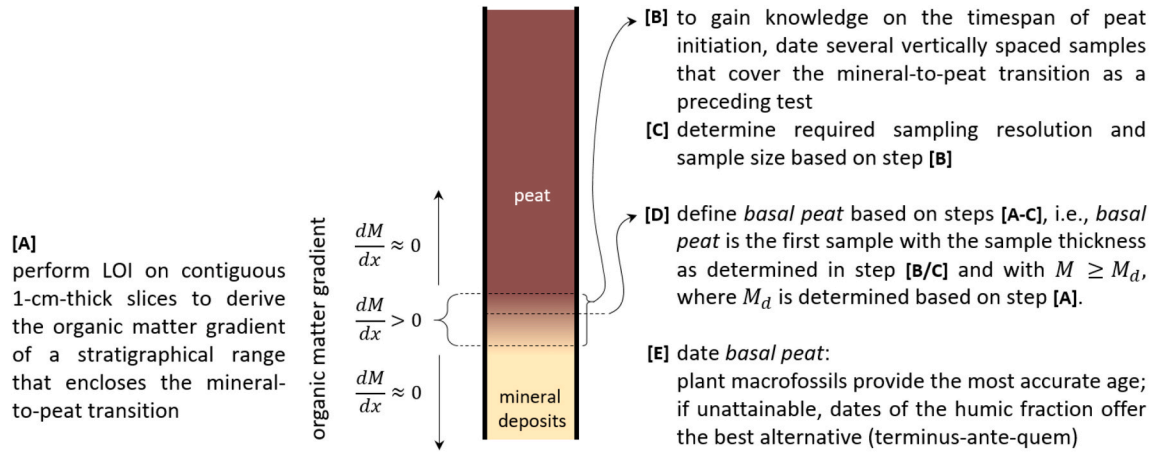

results. If insufficient plant macrofossils are retrieved, the humic fraction provides the best alternative for dating, however dating results are most safely interpreted as a terminus-ante-quem for peat initiation. The potential large age difference between dates of plant macrofossils and humic or humin dates (up to ~1700 years between macrofossil and humic ages, and with even larger differences for humins) indicates that studies reusing existing bulk dates of *basal peat* should take great care in data interpretation. The potentially long timespan of the peat initiation process (with medians of ~1000, ~1300 and ~1500 years within our case study peatland) demonstrates that choices regarding sampling size and resolution need to be well substantiated. Our findings are summarised as a set of recommendations for dating *basal peat* in textbox 1.

### 5.2. Palaeoenvironment

Our case study peatland in the Netherlands currently harbours a bog vegetation, but biostratigraphical analyses show that during peat initiation the vegetation was mesotrophic. This vegetation was dominated by sedges, with some presence of *Juncus*. The data indicate that the peat initiation process initially involved fluctuating water tables and that wetter and drier conditions probably alternated. Frequent presence of charred plant remains demonstrates that wildfires occurred regularly. After the peat initiation process, conditions became more oligotrophic, and the vegetation developed probably to an oligotrophic bog with *Calluna vulgaris*, *Erica tetralix* and *Sphagnum* at two of the studied locations and to a moss (*Bryales*) and heather vegetation at the third location.

## Data availability

All data from this study are available at the 4TU.Centre for Research Data; see Quik et al. (2022).

## Author contributions

RvB secured funding for this research. CQ proposed the research outline, which was further improved based on feedback by JW, JC, BM, YvdV, and RvB. JC and CQ explored the study area, performed test corings and decided upon a coring strategy. CQ organised the fieldwork and completed the collection of data and cores in the field with help of several students (see acknowledgements). CQ coordinated all subsequent analyses that were performed on the obtained cores. Cores were opened and subsampled by MvdL and CQ. LK performed the microscopy work for analyses of plant macro remains and selection of datable material. MvdL interpreted and reported the resulting vegetation data. GS analysed the subsamples for testate amoebae. CQ performed the majority of LOI analyses, a small part of the subsamples were analysed by the CBLB (see acknowledgements). SP worked on the radiocarbon dating at the CIO laboratory in Groningen. All resulting data were combined and analysed by CQ. CQ wrote the main body of text, with input from the reports by MvdL and GS, and from discussions with JW, JC, BM, YvdV and RvB. The manuscript was finalized based on feedback from all authors.

## Declaration of competing interest

The authors declare that they have no known competing financial interests or personal relationships that could have appeared to influence the work reported in this paper.

## Acknowledgements

This research is part of the research programme *Home Turf - An integrated approach to Dutch raised bogs*, funded by the Netherlands Organization for Scientific Research (NWO) under grant number: 276-60-003. We thank Roos Veeneklaas (Natuurmonumenten Noordenveld) for permission to do fieldwork at the Fochteloërveen and for sharing detailed field knowledge; Hans Beens (Staatsbosbeheer Kop van Drenthe) for providing access to private roads to be able to reach the field sites; Teun Fiers, Klais Blaauw, Tom Harkema, Marte Stoorvogel, and Gibran Leeflang for field assistance; Mieke Hannink for administrative assistance with organising the fieldwork; Marcello Novani (Laboratory for Geo-information Science, WUR) for providing GNSS equipment; Jim Quik for construction work for core transport; Wouter van der Meer (BIAX Consult) for his help with opening and subsampling the cores; Harm Goorens for assistance with LOI analyses at the Soil Hydro Physics Lab (WUR) and Piet Peters for providing storage space in the cool room; Anne Roepert and colleagues of the CBLB for LOI analyses; Romy Koudijs for sharing OM data on the five duplicate cores; and Bas van Geel for his kind introduction to analysis of plant macrofossils. We thank Julie Loisel and an anonymous reviewer for their constructive comments to an earlier version of this manuscript; their feedback was much appreciated.

## References

Aaby, B., 1986. Palaeoecological studies of mires. In: Berglund, B.E. (Ed.), Handbook of Holocene Palaeoecology and Palaeohydrology. J. Wiley, Chichester; New York, pp. 145–164.

AHN, 2021a. De details van het Actueel Hoogtebestand Nederland [details of the digital elevation model of The Netherlands]. Available at: https://ahn.maps.arcgis.com/apps/Cascade/index.html?appid=75245be5e0384d47856d2b912fc1b7ed.

AHN, 2021b. Kwaliteitsbeschrijving Actueel Hoogtebestand Nederland [Quality Description Digital Elevation Model of The Netherlands. Available at: https://www.ahn.nl/kwaliteitsbeschrijving. (Accessed 11 October 2021).

Almquist-Jacobson, H., Foster, D.R., 1995. Toward an integrated model for raised-bog development: theory and field evidence. Ecology 76 (8), 2503–2516. https://doi.org/10.2307/2265824.

Anderberg, A.-L., 1994. Atlas of seeds and small fruits of Northwest-European plant species; Part 4: resedaceae-umbelliferae. In: The Swedish Natural Science Research Council. Statens naturvetenskapliga forskningaråd, Stockholm.

Bayliss, A., 2009. Rolling out revolution: using radiocarbon dating in archaeology. Radiocarbon 51 (1), 123–147.

Bayliss, A., McCormac, G., Van der Plicht, H., 2004. An illustrated guide to measuring radiocarbon from archaeological samples. Phys. Educ. 39 (2), 1–8. https://doi.org/10.1088/0031-9120/39/2/001.

Berendsen, H.J.A., Makaske, B., Van de Plassche, O., Van Ree, M.H.M., Das, S., Van Dongen, M., Ploumen, S., Schoenmakers, W., 2007. New groundwater-level rise data from the Rhine-Meuse delta - implications for the reconstruction of Holocene relative mean sea-level rise and differential land-level movements. Geologie en Mijnbouw/Neth. J. Geosci. 86 (4), 333–354. https://doi.org/10.1017/s0016774600023568.

Berggren, G., 1969. Atlas of seeds and small fruits of Northwest-European plant species; Part 2: cyperaceae. In: The Swedish Natural Science Research Council. Statens naturvetenskapliga forskningaråd, Stockholm.

Berggren, G., 1981. Atlas of seeds and small fruits of Northwest-European plant species; Part 3: salicaceae-cruciferae. In: The Swedish Natural Science Research Council. Statens naturvetenskapliga forskningaråd, Stockholm.

Blaauw, M., van der Plicht, J., van Geel, B., 2004. Radiocarbon dating of bulk peat samples from raised bogs: non-existence of a previously reported 'reservoir effect. Quat. Sci. Rev. 23, 1537–1542. https://doi.org/10.1016/j.quascirev.2004.04.002.

Booth, R.K., Lamentowicz, M., Charman, D.J., 2010. Preparation and analysis of testate amoebae in peatland palaeoenvironmental studies. Mires Peat 7 (2), 1–7.

Bos, I.J., 2010. Architecture and facies distribution of organic-clastic lake fills in the fluvio-deltaic Rhine-Meuse system, The Netherlands. J. Sediment. Res. 80, 339–356. https://doi.org/10.2110/jsr.2010.035.

Bos, I.J., Busschers, F.S., Hoek, W.Z., 2012. Organic-facies determination: a key for understanding facies distribution in the basal peat layer of the Holocene Rhine-Meuse delta, The Netherlands. Sedimentology 59 (2), 676–703. https://doi.org/10.1111/j.1365-3091.2011.01271.x.

Bosch, J.H.A., 1990. Assen West (12W), Assen Oost (12O). Toelichtingen bij de geologische kaart van Nederland 1:50.000. Rijks Geologische Dienst, Haarlem.

Breuning-Madsen, H., Bird, K.L., Balstrøm, T., Elberling, B., Kroon, A., Lei, E.B., 2018. Development of plateau dunes controlled by iron pan formation and changes in land use and climate. Catena 171, 580–587. https://doi.org/10.1016/j.catena.2018.07.011.

Brock, F., Lee, S., Housley, R.A., Bronk Ramsey, C., 2011. Variation in the radiocarbon age of different fractions of peat: a case study from Ahrenshöft, northern Germany. Quat. Geochronol. 6 (6), 550–555. https://doi.org/10.1016/j.quageo.2011.08.003.

Bronk Ramsey, C., 1995. Radiocarbon calibration and analysis of stratigraphy: the OxCal program. Radiocarbon 37 (2), 425–430. https://doi.org/10.1017/s0033822200030903.

Bronk Ramsey, C., 2008a. Radiocarbon dating: revolutions in understanding. Archaeometry 50 (2), 249–275. https://doi.org/10.1111/j.1475-4754.2008.00394.x.

Bronk Ramsey, C., 2008b. Deposition models for chronological records. Quat. Sci. Rev. 27, 42–60. https://doi.org/10.1016/j.quascirev.2007.01.019.

Bronk Ramsey, C., 2009. Dealing with outliers and offsets in radiocarbon dating. Radiocarbon 51 (3), 1023–1045. https://doi.org/10.1017/s0033822200034093.
Cappers, R.T.J., Bekker, R.M., Jans, J.E.A., 2006. Digitale Zadenatlas Van Nederland. Barkhuis Publishing & Groningen University Library, Eelde, Groningen.
Chambers, F.M., Beilman, D.W., Yu, Z., 2011. - Methods for determining peat humification and for quantifying peat bulk density. Mires Peat 7 (7), 1–10. Available at: http://www.mires-and-peat.net/pages/volumes/map07/map0707.php.
Chapman, H., Gearey, B.R., Bamforth, M., Bermingham, N., Marshall, P., Powlesland, I., Taylor, M., Whitehoude, N., 2013. Modelling archaeology and palaeoenvironments in wetlands: the hidden landscape archaeology of Hatfield and Thorne Moors, eastern England. Available at: https://www.oxbowbooks.com/oxbow/modelling-archaeology-and-palaeoenvironments-in-wetlands.html.
Charman, D., 2002a. Peat and peatlands. In: Charman, D. (Ed.), Peatlands and Environmental Change. John Wiley & Sons, Ltd, Chichester, pp. 3–23.
Charman, D., 2002b. Origins and peat initiation. In: Charman, D. (Ed.), Peatlands and Environmental Change. John Wiley & Sons, Ltd, Chichester, pp. 73–91.
Charman, D., 2002c. Autogenic change. In: Charman, D. (Ed.), Peatlands and Environmental Change. John Wiley & Sons, Ltd, Chichester, pp. 143–165.
Cook, G.T., Dugmore, A.J., Shore, J.S., 1998. The influence of pretreatment on humic acid yield and 14C age of carex peat. Radiocarbon 40 (1), 21–27. https://doi.org/10.1017/s0033822200017835.
Cubizolle, H., Bonnel, P., Oberlin, C., Tourman, A., Porteret, J., 2007. Advantages and limits of radiocarbon dating applied to peat inception during the end of the Late Glacial and the Holocene: the example of mires in the eastern Massif Central (France). Quaternaire 18 (2), 187–208. https://doi.org/10.4000/quaternaire.1049.
De Bakker, H., Schelling, J., 1966. Systeem Van Bodemclassificatie Voor Nederland: De Hogere Niveaus. Stichting voor Bodemkartering, Pudoc: Wageningen.
De Vleeschouwer, F., Chambers, F.M., Swindles, G.T., 2010. Coring and sub-sampling of peatlands for palaeoenvironmental research. Mires Peat 7, 1–10.
Dee, M.W., Palstra, S.W.L., Aerts-Bijma, A.T., Bleeker, M.O., De Bruijn, S., Ghebru, F., Jansen, H.G., Kuitems, M., Paul, D., Richie, R.R., et al., 2020. Radiocarbon dating at Groningen: new and updated chemical pretreatment procedures. Radiocarbon 62 (1), 63–74. https://doi.org/10.1017/RDC.2019.101.
Douwes, R., Straathof, N., 2019. 14. Het Fochteloërveen. In: Herstel, Jansen A., Grootjans, A. (Eds.), Hoogvenen: Landschapsecologie, Behoud, Beheer, Noordboek Natuur: Gorredijk, pp. 133–147.
Drenthe, Provincie, 2016. Beheerplan Fochteloërveen - Op Weg Naar Een Levend Hoogveen. Provincie Drenthe, Assen.
Edvardsson, J., Poska, A., Van der Putten, N., Rundgren, M., Linderson, H., Hammarlund, D., 2014. Late-Holocene expansion of a south Swedish peatland and its impact on marginal ecosystems: evidence from dendrochronology, peat stratigraphy and palaeobotanical data. Holocene 24 (4), 466–476. https://doi.org/10.1177/0959683613520255.
Eijkelkamp Agrisearch Equipment, 2022. Percussion Drilling Equipment: 1–4. Available at: https://en.eijkelkamp.com/products/augering-soil-sampling-equipment/percussion-drilling-set-gasoline-percussion-hammer.html. (Accessed 16 February 2022).
Eijkelkamp Soil & Water, 2018. Peat sampler. Eijkelkamp soil & water, giesbeek. Available at: http://www.vanwalt.com/sediment-sampling-gouges-augers.html#PeatSamplerSet.
Gerding, M., 1995. Vier eeuwen turfwinning, De verveningen in Groningen, Friesland, Drenthe en Overijssel tussen 1550 en 1950. Wageningen University, Wageningen.
Givelet, N., Le Roux, G., Cheburkin, A., Chen, B., Frank, J., Goodsite, M.E., Kempter, H., Krachler, M., Noernberg, T., Rausch, N., et al., 2004. Suggested protocol for collecting, handling and preparing peat cores and peat samples for physical, chemical, mineralogical and isotopic analyses. J. Environ. Monit. 6, 481–492. https://doi.org/10.1039/b401601g.
Goh, K.M., Molloy, B.P.J., 1978. Radiocarbon dating of paleosols using soil organic matter components. J. Soil Sci. 29, 567–573. https://doi.org/10.1111/j.1365-2389.1978.tb00805.x.
Gorham, E., Lehman, C., Dyke, A., Janssens, J., Dyke, L., 2007. Temporal and spatial aspects of peatland initiation following deglaciation in North America. Quat. Sci. Rev. 26 (3–4), 300–311. https://doi.org/10.1016/j.quascirev.2006.08.008.
Hammond, A.P., Goh, K.M., Tonkin, P.J., Manning, M.R., 1991. Chemical pretreatments for improving the radiocarbon dates of peats and organic silts in a gley podzol environment: grahams Terrace, North Westland. N. Z. J. Geol. Geophys. 34, 191–194. https://doi.org/10.1080/00288306.1991.9514456.
Holmquist, J.R., Finkelstein, S.A., Garneau, M., Massa, C., Yu, Z., MacDonald, G.M., 2016. A comparison of radiocarbon ages derived from bulk peat and selected plant macrofossils in basal peat cores from circum-arctic peatlands. Quat. Geochronol. 31, 53–61. https://doi.org/10.1016/j.quageo.2015.10.003.
Hughes, P.D.M., 2000. A reappraisal of the mechanisms leading to ombrotrophy in British raised mires. Ecol. Lett. 3, 7–9. https://doi.org/10.1046/j.1461-0248.2000.00118.x.
Hughes, P.D.M., Barber, K.E., 2004. Contrasting pathways to ombrotrophy in three raised bogs from Ireland and Cumbria, England. Holocene 14 (1), 65–77. https://doi.org/10.1191/0959683604hl690rp.
Iversen, C.M., Sloan, V.L., Sullivan, P.F., Euskirchen, E.S., Mcguire, A.D., Norby, R.J., Walker, A.P., Warren, J.M., Wullschleger, S.D., 2015. The unseen iceberg: plant roots in arctic tundra. New Phytol. 205, 34–58. https://doi.org/10.1111/nph.13003.
Joosten, H., Clarke, D., 2002. Wise Use of Mires and Peatlands - Background and Principles Including a Framework for Decision-Making. International Mire Conservation Group (IMCG) & International Peatland Society (IPS).
Jull, A., Burr, G., 2015. Accelerator mass spectrometry. In: Encyclopedia of Scientific Dating Methods, pp. 3–6. https://doi.org/10.1007/978-94-007-6304-3.
Kennedy, D.M., Woods, J.L.D., 2013. Determining Organic and Carbonate Content in Sediments. Elsevier Ltd. https://doi.org/10.1016/B978-0-12-374739-6.00389-4.
Kilian, M., van der Plicht, J., van Geel, B., 1995. Dating raised bogs: new aspects of AMS 14C wiggle matching, a reservoir effect and climatic change. Quat. Sci. Rev. 14, 959–966.
KNMI, 2021. Klimaattabel Station Eelde, Periode 1991-2020: 1.
Kohzu, A., Matsui, K., Yamada, T., Sugimoto, A., Fujita, N., 2003. Significance of rooting depth in mire plants: evidence from natural 15N abundance. Ecol. Res. 18, 257–266. https://doi.org/10.1046/j.1440-1703.2003.00552.x.
Körber-Grohne, U., 1964. Bestimmungsschlüssel für subfossile Juncus-Samen und Gramineen-Früchte. Hildesheim.
Körber-Grohne, U., 1991. Bestimmungsschlüssel für subfossile Gramineen-Früchte. Probl. Kustenforsch. Sudlichen Nord. 18.
Korhola, A., 1994. Radiocarbon evidence for rates of lateral expansion in raised mires in southern Finland. Q. Res. 42, 299–307.
Koster, E.A., 1988. Ancient and modern cold-climate aeolian sand deposition: a review. J. Quat. Sci. 3, 69–83.
Koster, E., 2005. Aeolian environments. In: Koster, E.A. (Ed.), Physical Geography of Western Europe. Oxford University Press, Oxford, pp. 139–160.
Loisel, J., Bunsen, M., 2020. Abrupt fen-bog transition across southern Patagonia: timing, causes, and impacts on carbon sequestration. Front. Ecol. Evol. 8, 1–19. https://doi.org/10.3389/fevo.2020.00273.
Loisel, J., Yu, Z., Parsekian, A., Nolan, J., Slater, L., 2013. Quantifying landscape morphology influence on peatland lateral expansion using ground-penetrating radar (GPR) and peat core analysis. J. Geophys. Res.: Biogeosciences 118, 373–384. https://doi.org/10.1002/jgrg.20029.
Macdonald, G.M., Beilman, D.W., Kremenetski, K.V., Sheng, Y., Smith, L.C., Velichko, A. A., 2006. Rapid early development of circumarctic peatlands and atmospheric CH4 and CO2 variations. Science 314, 285–288. https://doi.org/10.1126/science.1131722.
Mäkilä, M., 1997. Holocene lateral expansion, peat growth and carbon accumulation on Haukkasuo, a raised bog in southeastern Finland. Boreas 26 (1), 1–14. https://doi.org/10.1111/j.1502-3885.1997.tb00647.x.
Mäkilä, M, Moisanen, M, 2007. Holocene lateral expansion and carbon accumulation of Luovuoma, a northern fen in finnish Lapland. Boreas 36 (2), 198–210. https://doi.org/10.1111/j.1502-3885.2007.tb01192.x.
Ministerie van Economische Zaken, 2018. Natura 2000-gebieden Peildatum 27 Augustus 2018 [Data File].
Ministerie van Verkeer en Waterstaat, 2007. Landelijke CONCEPT Dataset Lijnvormige Waterlichamen Status Mrt 2007 [Data File].
Moore, P.D., 1975. Origin of blanket mires. Nature 256 (5515), 267–269. https://doi.org/10.1038/256267a0.
Moore, P., 1993. The origin of blanket mire, revisited. In: Chambers, F. (Ed.), Climate Change and Human Impact on the Landscape. Chapman and Hal, London, pp. 217–224.
Morris, P.J., Swindles, G.T., Valdes, P.J., Ivanovic, R.F., Gregoire, L.J., Smith, M.W., Tarasov, L., Haywood, A.M., Bacon, K.L., 2018. Global peatland initiation driven by regionally asynchronous warming. Proc. Natl. Acad. Sci. U. S. A. 115 (19), 4851–4856. https://doi.org/10.1073/pnas.1717838115.
Nelson, K., Thompson, D., Hopkinson, C., Petrone, R., Chasmer, L., 2021. Peatland-fire interactions: a review of wildland fire feedbacks and interactions in Canadian boreal peatlands. Sci. Total Environ. 769, 1–14. https://doi.org/10.1016/j.scitotenv.2021.145212.
Nilsson, M., Klarqvist, M., Bohlin, E., Possnert, G., 2001. Variation in 14C age of macrofossils and different fractions of minute peat samples dated by AMS. Holocene 11 (5), 579–586. https://doi.org/10.1191/095968301680223521.
Palstra, S.W.L., Wallinga, J., Viveen, W., Schoorl, J.M., Van den Berg, M., Van der Plicht, J., 2021. Cross-comparison of last glacial radiocarbon and OSL ages using periglacial fan deposits. Quat. Geochronol. 61 https://doi.org/10.1016/j.quageo.2020.101128.
Philippsen, B., 2013. The freshwater reservoir effect in radiocarbon dating. Herit. Sci. 1 (24), 1–19. https://doi.org/10.1186/2050-7445-1-24.
Piotrowska, N., Blaauw, M., Mauquoy, D., Chambers, F., 2011. Constructing deposition chronologies for peat deposits using radiocarbon dating. Mires Peat 7, 1–14. Available at: http://www.mires-and-peat.net/map07/map_07_10.pdf.
Quik, C., Van der Velde, Y., Harkema, T., Van der Plicht, H., Quik, J., Van Beek, R., Wallinga, J., 2021. Using legacy data to reconstruct the past? Rescue, rigor and reuse in peatland geochronology. Earth Surf. Process. Landforms 46, 2607–2631. https://doi.org/10.1002/esp.5196.
Quik, C., Palstra, S.W.L., Van Beek, R., Van der Velde, Y., Candel, J.H.J., Van der Linden, M., Kubiak-Martens, L., Swindles, G., Makaske, B., et al., 2022. Data from: Dating basal peat: the geochronology of peat initiation revisited. 4TU.Centre for Research Data. doi: 10.4121/16923358.
Rappol, M., 1987. Saalian till in The Netherlands: a review. In: Van der Meer, J.J.M. (Ed.), INQUA Symposium on the Genesis and Lithology of Glacial Deposits – Amsterdam, 1986. Balkema, Rotterdam, Boston, pp. 3–21.
Rappol, M., Haldorsen, S., Jørgensen, P., Van der Meer, J.J.M., Stoltenberg, H.M.P., 1989. Composition and origin of petrographically stratified thick till in the Northern Netherlands and a Saalian glaciation model for the North Sea basin. Mededelingen van de Werkgroep voor Tertiair en Kwartair Geologie 26, 31–64.
Reimer, P., Austin, W., Bard, E., Bayliss, A., Blackwell, P., Bronk Ramsey, C., Butzin, M., Cheng, H., Edwards, R., Friedrich, M., et al., 2020. The IntCal20 Northern Hemisphere radiocarbon age calibration curve (0–55 cal kBP). Radiocarbon 62 (4), 725–757. https://doi.org/10.1017/RDC.2020.41.
Rein, G., Huang, X., 2021. Smouldering wildfires in peatlands, forests and the arctic: challenges and perspectives. Curr. Opin. Environ. Sci. Health. https://doi.org/10.1016/j.coesh.2021.100296.

Roe, H.M., Charman, D.J., Roland Gehrels, W., 2002. Fossil testate amoebae in coastal deposits in the UK: implications for studies of sea-level change. J. Quat. Sci. 17 (5–6), 411–429. https://doi.org/10.1002/jqs.704.
Ruppel, M., Väliranta, M., Virtanen, T., Korhola, A., 2013. Postglacial spatiotemporal peatland initiation and lateral expansion dynamics in North America and northern Europe. Holocene 23 (11), 1596–1606. https://doi.org/10.1177/0959683613499053.
Rydin, H., Jeglum, J.K., 2013a. Peatland habitats. In: Rydin, H., Jeglum, J.K. (Eds.), The Biology of Peatlands. Oxford University Press, Oxford, pp. 1–20.
Rydin, H., Jeglum, J.K., 2013b. Peatland succession and development. In: Rydin, H., Jeglum, J.K. (Eds.), The Biology of Peatlands. Oxford University Press, Oxford, pp. 127–147.
Rydin, H., Jeglum, J.K., 2013c. Productivity and peat accumulation. In: Rydin, H., Jeglum, J.K. (Eds.), The Biology of Peatlands. Oxford University Press, Oxford, pp. 254–273.
Shore, J.S., Bartley, D.D., Harkness, D.D., 1995. Problems encountered with the 14C dating of peat. Quat. Sci. Rev. 14 (4), 373–383. https://doi.org/10.1016/0277-3791(95)00031-3.
Smith, A.J., 2004. The Moss Flora of Britain and Ireland. Cambridge University Press, Cambridge.
Smolders, A.J.P., Tomassen, H.B.M., Pijnappel, H.W., Lamers, L.P.M., Roelofs, J.G.M., 2001. Substrate-derived CO2 is important in the development of Sphagnum spp. New Phytol. 152 (2), 325–332. https://doi.org/10.1046/j.0028-646X.2001.00261.x.
Straathof, N., Bijkerk, W., Land, K.A., 2017. Neergang en opkomst van het Fochteloërveen : resu ltaten van 30 iaar hoogveenherstel. July).
Streif, H., 1972. The results of stratigraphical and facial investigations in the coastal Holocene of Woltzeten/Ostfriesland, Germany. Geol. Foren. Stockh. Forh. 94 (2), 281–299. https://doi.org/10.1080/11035897209454203.
Stuiver, M, Polach, H, 1977. Discussion Reporting of 14C Data. Radiocarbon 19 (3), 355–363.
Sullivan, M.E., Booth, R.K., 2011. The potential influence of short-term environmental variability on the composition of testate amoeba communities in Sphagnum peatlands. Microb. Ecol. 62 (1), 80–93.
Swindles, G.T., Roe, H.M., 2007. Examining the dissolution characteristics of testate amoebae (Protozoa: rhizopoda) in low pH conditions: implications for peatland palaeoclimate studies. Palaeogeogr. Palaeoclimatol. Palaeoecol. 252 (3–4), 486–496. https://doi.org/10.1016/j.palaeo.2007.05.004.
Swindles, G.T., Roland, T.P., Amesbury, M.J., Lamentowicz, M., McKeown, M.M., Sim, T. G., Fewster, R.E., Mitchell, E.A.D., 2020. Quantifying the effect of testate amoeba decomposition on peat-based water-table reconstructions. Eur. J. Protistol. 74, 125693. https://doi.org/10.1016/j.ejop.2020.125693.
Synal, H.A., Stocker, M., Suter, M., 2007. MICADAS: a new compact radiocarbon AMS system. Nucl. Instrum. Methods B259, 7–13.
Ter Wee, M., 1972. Geologische Opbouw Van Drenthe. Rijks Geologische Dienst, Haarlem.
Ter Wee, M., 1979. Emmen West (17W), Emmen Oost (17O). Toelichtingen bij de geologische kaart van Nederland 1:50.000. Rijks Geologische Dienst, Haarlem.
TNO-GSN, 2021a. Basisveen bed. Stratigraphic Nomenclature of the Netherlands Available at: http://www.dinoloket.nl/en/stratigraphic-nomenclature/basis veen-bed. (Accessed 16 March 2021).
TNO-GSN, 2021b. Gieten member. Stratigraphic Nomenclature of the Netherlands Available at: http://www.dinoloket.nl/en/stratigraphic-nomenclature/giet en-member. (Accessed 1 April 2021).
TNO-GSN, 2021c. Laagpakket van Wierden. In: Stratigrafische Nomenclator Van Nederland. Available at: https://www.dinoloket.nl/en/stratigraphic-nomenclature/wierden-member. (Accessed 16 March 2021).
Tolonen, K., Turunen, J., 1996. Accumulation rates of carbon in mires in Finland and implications for climate change. Holocene 6 (2), 171–178. https://doi.org/10.1177/095968369600600204.
TOPCON, 2017. Hiper V Versatile Function GNSS Receiver. TOPCON Corporation.
Törnqvist, T.E., Hijma, M.P., 2012. Links between early Holocene ice-sheet decay, sea-level rise and abrupt climate change. Nat. Geosci. 5 (9), 601–606. https://doi.org/10.1038/ngeo1536.
Törnqvist, T.E., De Jong, A.F.M., Oosterbaan, W.A., Van Der Borg, K., 1992. Accurate dating of organic deposits by AMS 14C measurement of macrofossils. Radiocarbon 34 (3), 566–577. https://doi.org/10.1017/S0033822200063840.
Törnqvist, T.E., Van Ree, M.H.M., Van 't Veer, R., Van Geel, B., 1998. Improving methodology for high-resolution reconstruction of sea-level rise and neotectonics by paleoecological analysis and AMS 14C dating of basal peats. Q. Res. 49, 72–85. https://doi.org/10.1006/qres.1997.1938.
Törnqvist, T.E., Rosenheim, B.E., Hu, P., Fernandez, A.B., 2015. Radiocarbon dating and calibration. In: Shennan, I., Long, A.J., Horton, B.P. (Eds.), Handbook of Sea-Level Research. John Wiley & Sons, Ltd, pp. 349–360. https://doi.org/10.1002/9781118452547.ch23.
Tuniz, C., Bird, J.R., Fink, D., Herzog, G.F., 1998. Accelerator Mass Spectrometry: Ultrasensitive Analysis for Global Science. CRC Press, Boca Raton.
Väliranta, M., Salojärvi, N., Vuorsalo, A., Juutinen, S., Korhola, A., Luoto, M., Tuittila, E. S., 2017. Holocene fen–bog transitions, current status in Finland and future perspectives. Holocene 27 (5), 752–764. https://doi.org/10.1177/0959683616670471.
Van Aalst, J.W., 2021. OpenSimpleTopo, 3200 Pixels Per Km (Scale 1:3,125 as Hardcopy), Current Release: 2021-R02, Feb. 2021, Map Sheets Used: 3200-11HNb, 3200-11HNd, 3200-11HZb, 3200-12CNa, 3200-12CNb, 3200-12CNc, 3200-12CNd, 3200-12CZa, 3200-12CZb. Available at: www.opentopo.nl. (Accessed 19 May 2021).
Van Asselen, S., Cohen, K.M., Stouthamer, E., 2017. The impact of avulsion on groundwater level and peat formation in delta floodbasins during the middle-Holocene transgression in the Rhine-Meuse delta, The Netherlands. Holocene 27 (11), 1694–1706. https://doi.org/10.1177/0959683617702224.
Van Beek, R., Maas, G.J., Van Den Berg, E., 2015. Home Turf: an interdisciplinary exploration of the long-term development, use and reclamation of raised bogs in The Netherlands. Landsc. Hist. 36 (2), 5–34. https://doi.org/10.1080/01433768.2015.1108024.
Van den Berg, M.W., Beets, D.J., 1987. Saalian glacial deposits and morphology in The Netherlands. In: Van der Meer, J.J.M. (Ed.), INQUA Symposium on the Genesis and Lithology of Glacial Deposits – Amsterdam, 1986. Balkema, Rotterdam, Boston, pp. 235–251.
Van der Meij, W.M., Temme, A.J.A.M., Lin, H.S., Gerke, H.H., Sommer, M., 2018. On the role of hydrologic processes in soil and landscape evolution modeling: concepts, complications and partial solutions. Earth Sci. Rev. 185, 1088–1106. https://doi.org/10.1016/j.earscirev.2018.09.001.
Van der Plicht, J., Streurman, H., Van Mourik, J., 2019. Radiocarbon dating of soil archives. In: Van Mourik, J., Van der Meer, J. (Eds.), Reading the Soil Archives - Unravelling the Geoecological Code of Palaeosols and Sediment Cores (Developments in Quaternary Science 18). Elsevier B.V., pp. 81–113
Van Geel, B., 1978. A palaeoecological study of holocene peat bog sections in Germany and The Netherlands, based on the analysis of pollen, spores and macro- and microscopic remains of fungi, algae, cormophytes and animals. Rev. Palaeobot. Palynol. 25 (1), 1–120. https://doi.org/10.1016/0034-6667(78)90040-4.
Van Mourik, J., Wartenbergh, P., Mook, W., Streurman, H., 1995. Radiocarbon dating of palaeosols in aeolian sands. Meded. Rijks Geol. Dienst 52, 425–439.
Vos, P., De Vries, S., 2013. 2e generatie palaeogeografische kaarten van Nederland (versie 2.0. Available at: www.cultureelerfgoed.nl. (Accessed 22 January 2020).
Vos, P., Van der Meulen, M., Weerts, H., Bazelmans, J., 2020. Atlas of the Holocene Netherlands, Landscape and Habitation since the Last Ice Age. Amsterdam University Press, Amsterdam.
Waddington, J.M., Roulet, N.T., 1997. Groundwater flow and dissolved carbon movement in a boreal peatland. J. Hydrol. 191 (1–4), 122–138. https://doi.org/10.1016/S0022-1694(96)03075-2.
Waller, M.P., Long, A.J., Schofield, J.E., 2006. Interpretation of radiocarbon dates from the upper surface of late-Holocene peat layers in coastal lowlands. Holocene 16 (1), 51–61. https://doi.org/10.1191/0959683606hl895ra.
Wallinga, J., Van der Staay, J., 1999. Sampling in waterlogged sands with a simple hand-operated corer. Ancient TL 17, 59–61.
Weckström, J., Seppä, H., Korhola, A., 2010. Climatic influence on peatland formation and lateral expansion in sub-arctic Fennoscandia. Boreas 39 (4), 761–769. https://doi.org/10.1111/j.1502-3885.2010.00168.x.
Wohlfarth, B., Skog, G., Possnert, G., Holmquist, B., 1998. Pitfalls in the AMS radiocarbon-dating of terrestrial macrofossils. J. Quat. Sci. 13 (2), 137–145. https://doi.org/10.1002/(SICI)1099-1417(199803/04)13:2<137::AID-JQS352>3.0. CO;2-6.
WRB-IUSS, 2015. World Reference Base for Soil Resources. World Soil Resources Reports 106.
Wüst, R.A.J., Jacobsen, G.E., van der Gaast, H., Smith, A.M., 2008. Comparison of radiocarbon ages from different organic fractions in tropical peat cores: insights from Kalimantan, Indonesia. Radiocarbon 50 (3), 359–372. https://doi.org/10.1017/S0033822200053492.
Yu, Z., Beilman, D.W., Frolking, S., MacDonald, G.M., Roulet, N.T., Camill, P., Charman, D.J., 2011. Peatlands and their role in the global carbon cycle. Eos 92 (12), 1–3.
Zaccone, C., Rein, G., Orazio, V.D., Hadden, R.M., Belcher, C.M., Miano, T.M., 2014. Smouldering fire signatures in peat and their implications for palaeoenvironmental reconstructions. Geochem. Cosmochim. Acta 137, 134–146. https://doi.org/10.1016/j.gca.2014.04.018.